5-21-2022

Feasibility of Obtaining Surface Layer Moisture Flux Using an IR Thermometer

Steven T. Fiorino
Air Force Institute of Technology

Lance Todorowski
Applied Research Solutions, Beavercreek, Ohio

Jaclyn Schmidt
Applied Research Solutions, Beavercreek, Ohio

Yogendra Raut
Applied Research Solutions, Beavercreek, Ohio

Jacob Margraf
University of Oklahoma

Recommended Citation

Fiorino, S., Todorowski, L., Schmidt, J., Raut, Y., Keefer, K., & Margraf, J. (2022). Feasibility of Obtaining Surface Layer Moisture Flux Using an IR Thermometer. Applied Sciences, 12(10), 5225. https://doi.org/10.3390/app12105225 *applied sciences*

MDPI

Article

Feasibility of Obtaining Surface Layer Moisture Flux Using an IR Thermometer

Steven Fiorino [1,*], Lance Todorowski [1,2,3], Jaclyn Schmidt [1,2], Yogendra Raut [1,2], Kevin Keefer [1,2] and Jacob Margraf [4]

1 Department of Engineering Physics, Air Force Institute of Technology, 2950 Hobson Way, Dayton, OH 45433, USA; lance.todorowski.ctr@afit.edu (L.T.); jaclyn.schmidt.ctr@afit.edu (J.S.); yogendra.raut.ctr@afit.edu (Y.R.); kevin.keefer.ctr@afit.edu (K.K.)
2 Applied Research Solutions, 51 Plum Street, Suite 240, Beavercreek, OH 45440, USA
3 Department of Mechanical Engineering, University of Dayton, 300 College Park, Dayton, OH 45469, USA
4 School of Meteorology, University of Oklahoma, 120 David L Boren Blvd, Norman, OK 73072, USA; jacob.a.margraf-1@ou.edu
* Correspondence: steven.fiorino@afit.edu

Abstract: This paper evaluates the feasibility of a method using a single hand-held infrared (IR) thermometer and a mini tower of wet and dry paper towels to psychometrically obtain surface layer temperature and moisture gradients and fluxes. Sling Psychrometers have long been standard measuring devices for quantifying the thermodynamics of near-surface atmospheric gas–vapor mixtures, specifically moisture parameters. However, these devices are generally only used to measure temperature and humidity at one near-surface level. Multiple self-aspirating psychrometers can be used in a vertical configuration to measure temperature and moisture gradients and fluxes in the first 1–2 m of the surface layer. This study explores a way to make multiple vertical psychrometric measurements with a single non-contact IR temperature sensor rather than using two in situ thermometers at each level. The surface layer dry- and wet-bulb temperatures obtained using an IR Thermometer are compared to Kestrel 4000 Weather Meter and Bacharach Sling Psychrometer measurements under various atmospheric conditions and surface types to test the viability of the method. To evaluate the results obtained using this new approach, standard meteorological surface data are collected during each experiment, and moisture parameters are derived via psychrometric equations. The results indicate that, not only is the method possible and practical, but they suggest that the IR Thermometer method may provide more surface layer temperature and moisture gradient and flux sensitivity than other single instrument methods.

Keywords: infrared thermometer; wet-bulb temperature; moisture flux

Citation: Fiorino, S.; Todorowski, L.; Schmidt, J.; Raut, Y.; Keefer, K.; Margraf, J. Feasibility of Obtaining Surface Layer Moisture Flux Using an IR Thermometer. *Appl. Sci.* **2022**, *12*, 5225. https://doi.org/10.3390/app12105225

Academic Editor: Joao Carlos Andrade dos Santos

Received: 8 April 2022
Accepted: 18 May 2022
Published: 21 May 2022

1. Introduction

This study evaluates a method whereby a single non-contact infrared (IR) thermometer can be used to obtain both the vertical gradients and fluxes of air temperature and moisture content in the first 1–2 m of air above the ground. Since the IR Thermometer primarily quantifies the emissive temperature of material surfaces within its field of view (FOV), this paper outlines methods that allow the IR Thermometer to measure objects that are representative of the thermodynamic dry-bulb and wet-bulb temperatures. Standard psychrometric relationships and calculators can then be used with the obtained dry- and wet-bub temperatures (and pressure) to obtain standard meteorological quantifications of air temperature and humidity from a single IR Thermometer. The technique used in this experiment involves an IR Thermometer and paper towel material, along with a Kestrel 4000 Weather Meter and Sling Psychrometer for validation. Infrared thermometers are used to measure the temperature of the surface in the FOV within which the pointing laser (that typically is part of an IR Thermometer) is directed. A chief goal of this experiment is to establish how accurately a low-cost, procedurally simple, and relatively low maintenance IR Thermometer can quantify wet-bulb temperature when compared to standard psychrometric wet-bulb measurements and those derived from other moisture sensing devices.

The wet-bulb temperature, the temperature of an air parcel if cooled to a steady state via evaporation at constant pressure, provides a measure of the water vapor content of the air and is used to derive meteorological parameters, such as dew point temperature and relative humidity. Sling Psychrometers, (sometimes denoted as "Spsychrometers" or "Spsych" in this paper) are devices composed of two thermometers: one bulb is covered in a wet wick, whereas the other remains uncovered, utilized to quantify the physical and thermal properties of moist air. The dry-bulb temperature, which is essentially the ambient air temperature, is measured with the non-wick thermometer, whereas the wet-bulb temperature is obtained by evaporative cooling (a result of the slinging motion) of the moistened wick. To adequately measure the wet-bulb temperature, the psychrometer must be spun around at a speed of 2–3 revolutions per second for approximately 1.5–2 min until the wet-bulb thermometer reaches a constant value [1]. The World Meteorological Organization guidelines provide a broader range for acceptable ventilation rates, between 2.2 and 10 m s^{-1} [2]. Inconsistencies in measurements are generally associated with insufficient moistening of the cotton wick, low spin velocities or contaminated wicks. Furthermore, Sling Psychrometers can be affected by solar radiation, and measurements with direct sunlight on the thermometers during the ventilation process should be avoided. Additionally, to prevent physical damage to the device, measurements < 1 m above the ground are rarely performed.

The technique to use IR Thermometers is based on the same principles used by the Sling Psychrometer method and offers a fast, low risk and cost-effective method to measure temperature [3]. IR Thermometers exploit the property of all materials to emit electromagnetic radiation at temperatures above absolute zero [4]. The amount and primary wavelengths of the emitted energy are based on the temperature through Planck's Law [5–7]. IR Thermography is a measurement technique based on the detection of radiation in the IR spectrum, generally in the ranges of 2.0–5.6 and 8.0–14.0 μm [5]. These two spectral bands are commonly utilized because atmospheric absorption is relatively small, thus enabling sufficient broadband radiation to reach the sensor. In turn, the temperature of a radiating surface can be inferred from the Stefan–Boltzmann equation [6–8], as shown in Equation (1):

$$Emitted\ Energy = \epsilon \sigma T^4, \tag{1}$$

where T is the temperature (K) of the emitting surface, σ is the Stefan–Boltzmann constant = 5.67×10^{-8} W m^{-2} K^{-4} and ϵ is the wavelength-dependent emissivity of the radiating surface. Emissivity is an expression used to characterize the optical properties of materials, in this case wet or dry white paper towels, as a ratio of the amount of energy actually emitted to the amount emitted from an ideal blackbody at the same temperature. In such circumstances, the values for emissivity can be between 0 (i.e., perfect reflector, a mirror) and 1 (i.e., perfect emitter, blackbody). A concern about IR Thermography is that no IR detectors measure temperature directly; temperature is interpreted through emissivity. However, this concern is greatly reduced or eliminated if the emissivity of the material being investigated is ~1.0 in the spectral bands where the detector is sensitive [9].

To complete the assessment, the IR Thermometer technique was evaluated for efficiency and versatility. Experimental documentation entailed collecting data multiple times a day for several weeks in order to capture diurnal changes and various atmospheric conditions. Data were collected over sand, grass and concrete surfaces to establish if there were any significant differences in how accurately an IR Thermometer measures air temperature over those various surfaces as compared to other methods. The technique's versatility was also evaluated relative to freezing conditions to evaluate the use of an IR Thermometer for measuring ice-bulb temperature and converting that to humidity quantifications. Ultimately, the research explored the viability of using a single IR Thermometer to profile temperature and humidity at different heights in the first meter above the ground to describe moisture and heat fluxes near the surface.

Perhaps the strongest example of previous efforts illustrating the merit of this new technique for standard atmospheric humidity measurements is that which was reported by Lee and Wang [10]. In their work, they used non-contact IR Thermometers to advance commercial digital psychrometers normally installed in greenhouses to monitor ambient conditions with the primary focus of reducing the logistics footprint associated with such psychrometers. The psychrometers described by Lee and Wang—based on a captive moist wick coupled to a water reservoir—must be checked by personnel on a recurring basis with little to no foreknowledge that the reservoir is at a satisfactory operating level. Lee and Wang subsequently developed an elegant evaporative model based on monitoring the internal wick's wet-bulb temperature as determined by pointing a digital IR Thermometer at the wick and used that information to cue users when it was time to re-fill the internal water reservoir.

2. Methodology

2.1. Experimentation

In this research, the dry-bulb temperature was measured by pointing a Centech infrared thermometer at a dry paper towel approximately 15 cm away, a distance in which the paper towel completely fills the measurement spot defined by the Centech's optical resolution [3]. By ensuring the paper towel completely filled the viewed spot, there was no additional thermal radiation sampled from the background environment, which could degrade the accuracy of the temperature measurement. To measure the wet-bulb temperature, the paper towel was wetted with water, and a handheld fan was oriented perpendicular to it to maintain airflow into the wet towel for up to 1 min to create proper ventilation and thus evaporative cooling. Similar to the guidelines associated with accurate Sling Psychrometer measurements, IR Thermometer data were collected in shaded conditions to avoid sunlight contamination.

Experiments were conducted during the summer of 2020 near the University of Dayton campus, located in Dayton OH (39.7589° N, 84.1916° W). Dry- and wet-bulb temperatures were measured in various atmospheric conditions and over various surfaces (e.g., grass, concrete, sand), which influence those same atmospheric conditions. Experiments were conducted at different times of day and sky cover, as well as during rain events, to determine the applicability and limitations of the IR Thermometer technique. Simultaneous measurements were collected with a Bacharach Sling Psychrometer and Kestrel 4000 Weather Meter, which are shown in Figure 1. These instruments provided validation data. Dew point temperature, relative humidity and barometric pressure data were also collected by the Kestrel for comparisons to parameters measured and derived by the IR Thermometer and psychrometer. Relative humidity and dew point temperature were evaluated using psychrometric relationships and Bolton's equation (covered in Section 2.2).

Data collection procedures consisted of measuring atmospheric variables (e.g., dry-, wet-bulb temperature, pressure, relative humidity) with a Kestrel, followed directly with the IR Thermometer and Sling Psychrometer. Initial trials were conducted with a two-person team under a covered patio. While one individual held the paper and directed the airflow from the handheld fan toward the paper towel, the other person took temperature measurements by pointing the IR Thermometer at the center of the paper towel from approximately 15 cm away. Sling Psychrometer measurements were made by spinning the device around for approximately two minutes at the same height above the ground in which the paper towel was held.

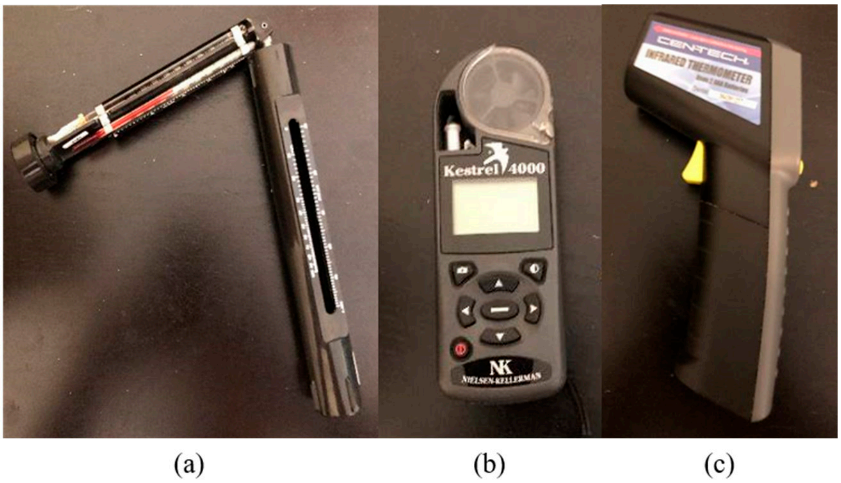

Figure 1. Images of the instrumentation used to conduct and validate the infrared psychrometry experiment: (**a**) Control: Bacharach 0012-7012 Sling Psychrometer; (**b**) Control: Kestrel 4000 Weather Meter, and (**c**) Test: Centech infrared thermometer (also known as IR Thermometer).

Experiments were conducted in an outdoor, open environment. Shade was found to be a critical prerequisite, as is generally sought for psychrometer measurements, to ensure that sunlight and thus solar heating did not affect the data. The instrumentation required time to become acclimated to the surrounding environment; it was noted that the IR sensor yielded inaccurate measurements after being relocated from a warm to a cool environment or vice versa [3]. Eventually the experimental setup was modified to require only one individual to conduct measurements; this was conducted by securing paper towels to the arms and base of a lawn chair while allowing for unobstructed air flow from the fan to create evaporative cooling. The measurements were organized by surface type and were originally made by one device (e.g., Kestrel) over all three surfaces in succession prior to switching to another device. Subsequently, procedural modifications were made to measure temperatures above a surface with all three (i.e., Kestrel, Sling Psychrometer and IR Thermometer) instruments in succession prior to moving to another surface. This modification reduced data inconsistencies due to environmental changes occurring during the measurement period. Sand surface experiments were conducted on an on-campus volleyball court, where an umbrella was deployed to create a shaded environment. The total time required to take all measurements over the various surfaces was approximately 30 min; therefore, environmental changes that occurred over the measurement cycle created subtle yet occasionally noticeable differences in data.

As noted earlier, the IR Thermometer technique was applied during freezing conditions to evaluate the capability to measure ice-bulb temperature (trials 54–62 in Appendix A). Numerous attempts were made to use a walk-in freezer for testing; however, due to COVID-19 restrictions, this option was not available for experimental analysis. Therefore, experiments were conducted in the freezer of a standard-sized refrigerator. A Sling Psychrometer was not used due to limitations of the freezer space. The Kestrel and wet paper towel were placed in the freezer with the door closed for 45 s to acclimate to the extreme temperatures. Ice-bulb temperature was measured first with the IR Thermometer after opening the door to limit warm, higher moisture air intrusion into the freezer environment. However, this often yielded wet-bulb temperatures that exceeded the dry-bulb measurements, presumably due to deposition and/or condensation on the wet/frozen paper towel that resulted in latent heat release on that towel that did not affect the dry paper towel or dry Kestrel moisture sensor nearly as much. Data from the Kestrel were quickly recorded after the ice-bulb temperature was measured. Although it is possible to have ice-bulb temperatures higher than the dry-bulb temperatures in environments saturated with respect to liquid water, the differing Kestrel/IR results strongly suggest that a walk-in freezer or below-freezing outdoor conditions are necessary to validate that the IR sensor technique can be applied in zero and sub-zero °C conditions.

The means and standard deviations of the measured dry-bulb and wet-bulb temperatures obtained from the three instruments over the three different surface types are shown in Figures 2–4. Note that the depicted daily mean and standard deviation temperature measurements derived by each method are superimposed on each method's final daily measurement. Results from preliminary trials demonstrated that the IR Thermometer technique could be utilized to quantify wet-bulb temperature and thus was expanded to determine its applicability to quantify vertical variations in wet-bulb temperatures, yielding a novel technique to measure moisture flux. As seen in Figure 5, paper towels were positioned on a wooden pole at several heights (i.e., 28, 46, 64, 81 and 99 cm) above ground level in a grassy, shaded area. As before, measurements were taken at various times of day and under varying sky conditions. The Kestrel was the only device used for validation measurements at each height, as the Sling Psychrometer is not a practical instrument to differentiate wet-bulb temperatures at relatively small height increments all within a meter of the ground.

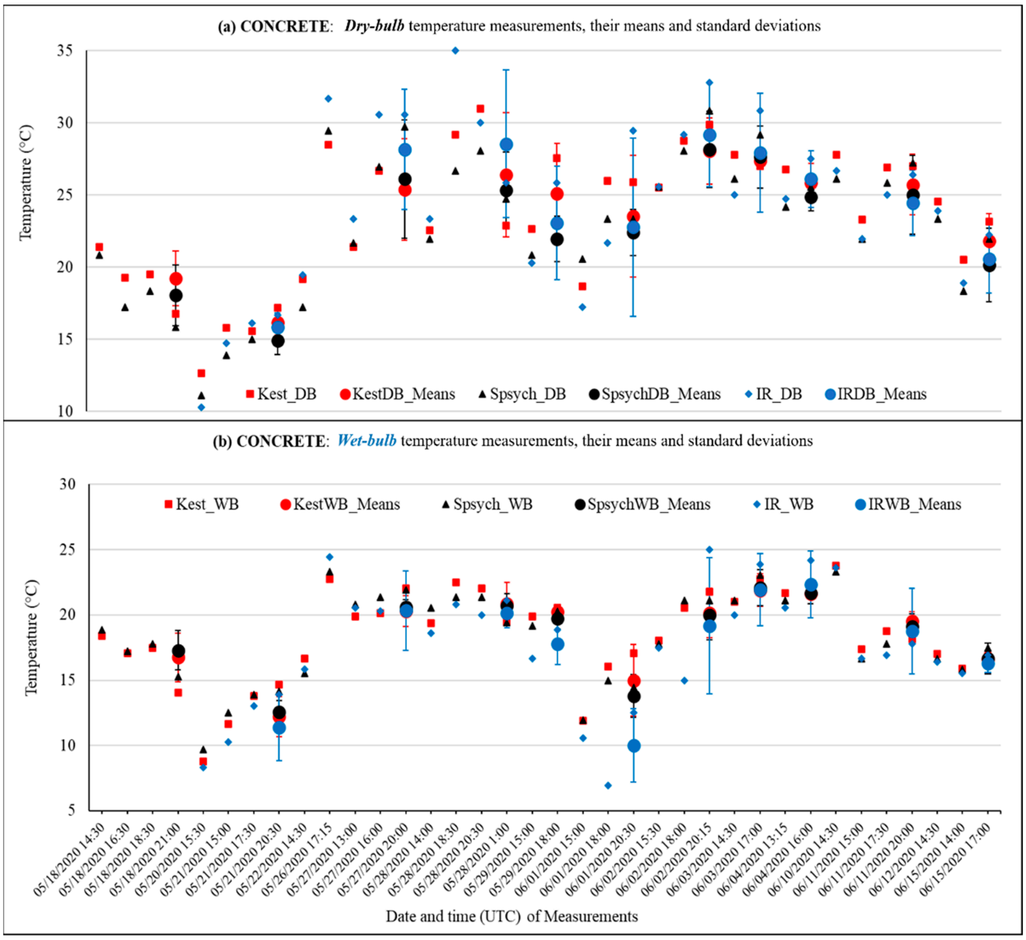

Figure 2. (**a**) Individual observations, as well as the daily means and standard deviations (superimposed on the final daily observation) of dry-bulb (DB) temperatures as measured by the Kestrel, Sling Psychrometer and IR Thermometer over concrete. (**b**) Individual observations, daily means, and standard deviations of wet-bulb (WB) temperatures as measured by the Kestrel, Sling Psychrometer and IR Thermometer over concrete.

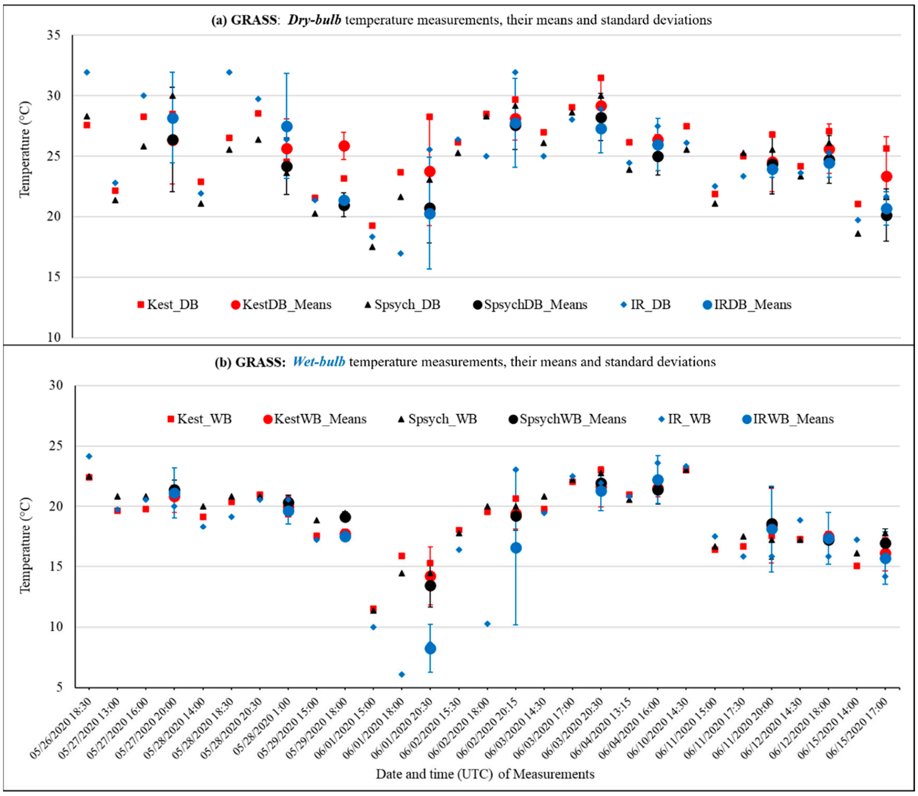

Figure 3. (**a**) Individual observations, as well as the daily means and standard deviations (superimposed on the final daily observation) of DB temperatures measured by the Kestrel, Sling Psychrometer and IR Thermometer over grass. (**b**) Individual observations, daily means and standard deviations of WB temperatures measured by the Kestrel, Sling Psychrometer and IR Thermometer over grass.

2.2. Conversion to Relative Humidity and Dew Point Temperature

Relative humidity and dew point temperature can be calculated using psychrometric relationships based on data obtained from the IR Thermometer and Kestrel measurements. Assuming the same temperature and pressure, relative humidity is a ratio of the vapor pressure of the air to the saturation vapor pressure [11],

$$RH = \frac{e}{e_s}\,, \tag{2}$$

Bolton's equation [12] is used to determine the saturation vapor pressure (hPa):

$$e_s(T) = 6.112\exp\left(\frac{17.67T}{T+243.5}\right), \tag{3}$$

with T being dry-bulb temperature (°C) measured by the IR Thermometer. Vapor pressure is calculated using the psychrometric equation [13],

$$e = e_{T_w} + \frac{c_{pd}P}{L_v\varepsilon}(T_w - T)\,, \tag{4}$$

where c_{pd} is specific heat of dry air (J kg^{-1} K^{-1}) at constant pressure, P is the barometric pressure (hPa) measured by the Kestrel, L_v is the latent heat of vaporization (J kg^{-1}), ε is the molar mass of water over the molar mass of air (0.622), e is vapor pressure (hPa), e_{Tw} is the wet-bulb vapor pressure (hPa), T_w is the wet-bulb temperature (°C) and T is the ambient air or dry-bulb temperature (°C). Latent heat of vaporization tables were used to determine L_v values based on IR Thermometer measurements.

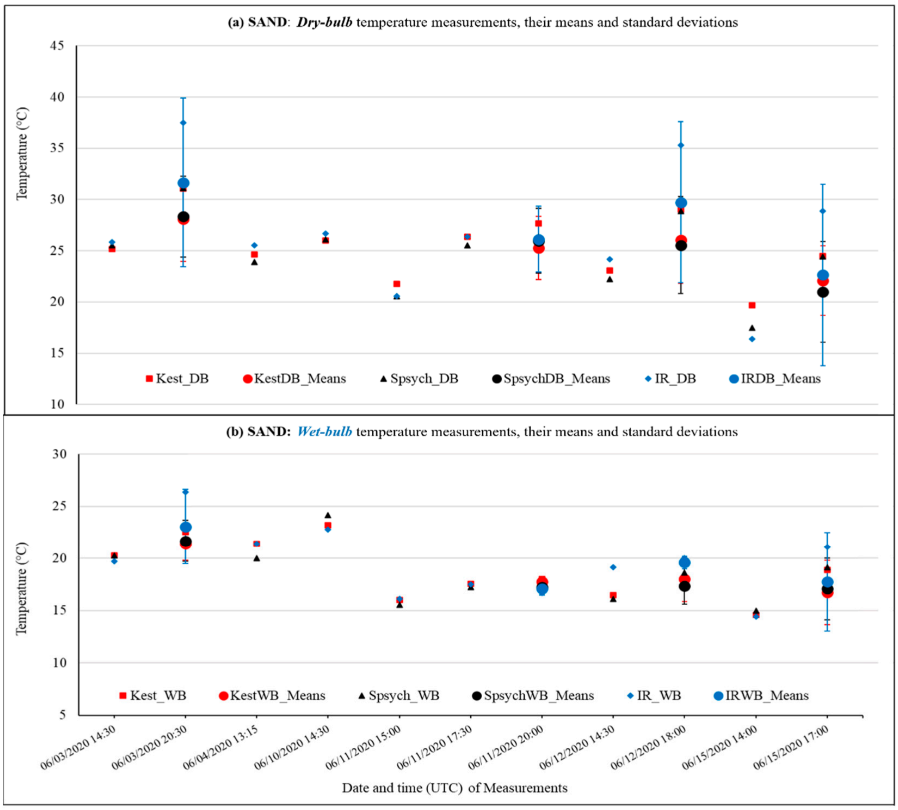

Figure 4. (**a**) Individual observations, as well as the daily means and standard deviations (superimposed on the final daily observation) of DB temperatures as measured by the Kestrel, Sling Psychrometer and IR Thermometer over sand. (**b**) Individual observations, daily means and standard deviations of wet-bulb (WB) temperature as measured by the Kestrel, Sling Psychrometer and IR Thermometer over sand.

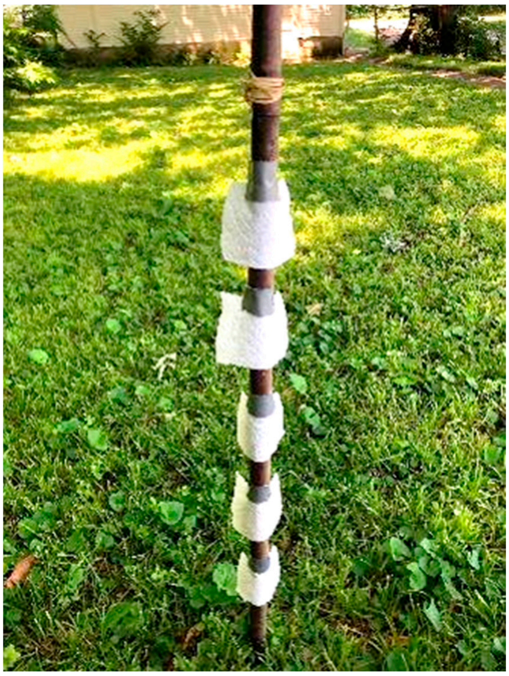

Figure 5. Moisture flux experimental setup consisting of small paper towels positioned at various heights (28, 46, 64, 81 and 99 cm) above a grassy surface.

Dew point temperature (T_d in °C), the temperature at which vapor pressure (or mixing ratio) and saturation vapor pressure (or saturation mixing ratio) are equivalent, is calculated using the vapor pressure from Equation (4) and the following equation [12]:

$$T_d = \frac{243.5 \ln\left(\frac{e}{6.112}\right)}{17.67 - \ln\left(\frac{e}{6.112}\right)}, \tag{5}$$

In addition to the measurements and equations outlined above, a USAF psychrometric whiz wheel calculator (ML-322/UM), shown in Figure 6, was used to validate the use of an empirical Clausius–Clapeyron Equation (5) to derive dew point temperature from the IR Thermometer's dry and wet-bulb temperature measurements. Relative humidity and vapor pressure are also outputs from the whiz wheel tool, which is an accurate representation of the full psychometric equations on a series of circular slide rules based on the following inputs: dry- and wet-bulb temperatures, as well as ambient atmospheric pressure. One limitation of the whiz wheel tool occurs with very large wet-bulb depressions (the $T_{drybulb}$—$T_{wetbulb}$ difference); this is due to the logarithmic nature of the scales and difficulty setting measurements on those scales.

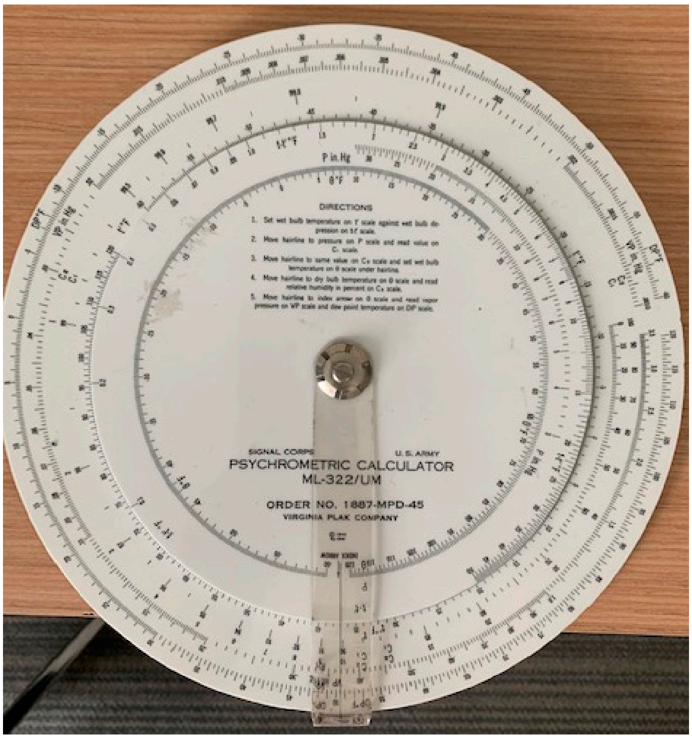

Figure 6. Psychrometric Calculator Model #ML-322/UM, provided by the United States Air Force.

2.3. Statistical Analyses

In order to calculate the estimated standard deviation for the means displayed as uncertainty bars in Figures 2–4 and to statistically compare the measurements recorded by the control and test group instruments, two statistical approaches were applied. Firstly, a paired *t*-test assuming equal variances was applied to the control group (i.e., Kestrel and Sling Psychrometer) measurements. Subsequently, a single factor/one-way analysis of variance (ANOVA) procedure using SAS/JMP statistical software was performed for multiple means comparisons between the control and test (i.e., IR Thermometer) groups. Both procedures—the paired *t*-test and ANOVA—were implemented for the grass, concrete and sand surfaces, separately. For probability testing and significance analysis, a 5% alpha (α) level was adopted.

3. Discussion of Statistical Analysis and Measurement Results

3.1. Paired t-Test for Controls (Kestrel and Sling Psychrometer) Assuming Equal Variances

The experiment was conducted for three different surface conditions, namely grass, concrete and sand surfaces. Table 1 shows the results of the paired *t*-test analysis of the Kestrel and Sling Psychrometer control group dry- and wet-bulb temperature measurements for ultimate assessment of the IR Thermometer test group measurements. By applying p (T ≤ t = 0.060) in the grassy area, the mean dry-bulb temperature values of 25.816 °C (Sdev, ±2.930) and 24.521 °C (Sdev, ±3.320), as measured by the Kestrel and Sling Psychrometer, respectively, are not significantly different for $\alpha \leq 0.05$. As further confirmation, the t-statistic value of 1.575 is not greater than the t-critical of 1.667 in Table 1. For concrete and sand surfaces, the values of p (T ≤ t) are 0.214 and 0.342, respectively. This, in turn, suggests that the Kestrel mean dry-bulb temperature measured over concrete of 23.668 (±4.640) °C and the mean of 22.770 (±4.930) °C derived using the Sling Psychrometer are not significantly different. Likewise, the mean dry-bulb temperature measurements over sand with the Kestrel and Sling Psychrometer of 25.364 °C (±3.240) and 24.747 °C (±3.750), respectively, are statistically equivalent. In aggregate, these conclusions are confirmed by noting that the corresponding concrete/sand t-statistics values (0.797 and 0.412) are less than the t-critical thresholds (1.667 and 1.725) for both the Kestrel and Sling Psychrometer; their dry-bulb temperature mean measurements over concrete and sand are effectively the same (Table 1).

Table 1. Paired *t*-test for a sample assuming equal variances between two control groups (Kestrel and Sling Psychrometer) measured for three different surfaces ($\alpha \leq 0.05$).

		Dry-Bulb Temperature (°C)		Wet-Bulb Temperature (°C)	
Surface Type	**Control Group**	**Kestrel**	**Sling Psych**	**Kestrel**	**Sling Psych**
Grass	Mean	25.816	24.521	18.910	19.128
	Sdev (±)	2.930	3.320	2.710	2.800
	t-stat	1.575		−0.302	
	p (T ≤ t) one-tail	0.060		0.382	
	t-critical one-tail	1.673		1.673	
Concrete	Mean	23.668	22.770	18.378	18.333
	Sdev (±)	4.640	4.930	3.500	3.470
	t-stat	0.797		0.055	
	p (T ≤ t) one-tail	0.214		0.478	
	t-critical one-tail	1.670		1.667	
Sand	Mean	25.364	24.747	18.944	18.763
	Sdev (±)	3.240	3.750	2.740	2.960
	t-stat	0.412		0.1469	
	p (T ≤ t) one-tail	0.342		0.441	
	t-critical one-tail	1.725		1.725	

In the case of wet-bulb temperature measurements, means of 18.910 °C (±2.710) versus 19.128 °C (±2.800), 18.378 °C (±3.500) versus 18.333 °C (±3.470) and 18.944 °C (±2.740) versus 18.763 °C (±2.960) are statistically the same with p (T ≤ t) values 0.382, 0.478 and 0.441 at given $\alpha \leq 0.05$ for both the controls for all three surfaces. The calculated values for t-stat (−0.302, 0.055, and 0.149) are found to be lower in all three conditions compared to the t-critical (1.673, 1.667 and 1.725), which suggests that the means for wet-bulb temperatures are the same from these two controls (Table 1).

3.2. Single Factor ANOVA for Three Devices for Multiple Means Comparisons

This section largely deals with analysis of variance for comparison of the controls (i.e., Kestrel and Sling Psychrometer) and test (i.e., IR Thermometer) groups for dry and wet-bulb temperatures measured above grass, concrete and sand surfaces, the details of which are shown in Table 2a,b.

Table 2. (**a**) Single factor ANOVA for the three devices (Kest_DB, Spsych_DB and IR_DB) comprising control and test groups showing *dry*-bulb temperatures (°C) for grass, concrete and sand surfaces ($p < 0.05$). SS = Sum of squares; df = Degrees of freedom; MS = Mean square; F = F-ratio. (**b**) Single factor ANOVA for three devices (Kest_WB, Spsych_WB and IR_WB) comprising the control and test groups showing *wet*-bulb temperature (°C) for grass, concrete and sand surfaces ($p < 0.05$). SS = Sum of squares; df = Degrees of freedom; MS = Mean square; F = F-ratio.

(a)

Summary					ANOVA ($p < 0.05$)						
Groups	**Count**	**Sum**	**Mean**	**Variance**	**Source of Variation**	**SS**	**df**	**MS**	**F**	***p*-Value**	**F Crit**
GRASS											
Kest_DB	30	779.72	25.991	9.196	Between Groups	24	2	12.153	**0.879**	**0.419**	**3.101**
Spsych_DB	30	742.22	24.741	12.106	Within Groups	1203	87	13.825			
IR_DB	30	767.22	25.574	20.173	Total	1227	89				
CONCRETE											
Kest_DB	36	852.056	23.668	21.485	Between Groups	48	2	24.127	**0.929**	**0.398**	**3.086**
Spsych_DB	36	819.722	22.770	24.261	Within Groups	2624	101	25.979			
IR_DB	32	782.500	24.453	32.992	Total	2627	103				
SAND											
Kest_DB	10	247.944	7.674		Between Groups	10	2	5.221	**0.367**	**0.696**	**3.354**
Spsych_DB	10	241.111	10.696		Within Groups	384	27	14.222			
IR_DB	10	255.556	24.297		Total	394	29				

(b)

Summary					ANOVA ($p < 0.05$)						
Groups	**Count**	**Sum**	**Mean**	**Variance**	**Source of Variation**	**SS**	**df**	**MS**	**F**	***p*-Value**	**F Crit**
GRASS											
Kest_WB	29	548.389	18.910	7.333	Between Groups	24	2	12.198	**1.015**	**0.367**	**3.105**
Spsych_WB	29	554.722	19.128	7.852	Within Groups	1009	84	12.015			
IR_WB	29	519.444	17.912	20.859	Total	1034	86				
CONCRETE											
Kest_WB	36	661.611	18.378	12.226	Between Groups	13	2	6.274	**0.417**	**0.660**	**3.086**
Spsych_WB	36	660.000	18.333	12.019	Within Groups	1521	101	15.056			
IR_WB	32	563.333	17.604	21.678	Total	1533	103				
SAND											
Kest_WB	11	208.389	18.944	7.533	Between Groups	4	2	1.977	**0.214**	**0.808**	**3.316**
Spych_WB	11	206.398	18.763	8.786	Within Groups	277	30	9.233			
IR_WB	11	215.278	19.571	11.379	Total	281	32				

Table 2a,b show dry-bulb (DB) and wet-bulb (WB) temperature measurements by the control instruments and test instrument groups over grass, concrete and sand surface areas. The means of the dry-bulb temperatures measured by the Kestrel and Sling Psychrometer (control groups) and by the IR Thermometer (test group) for grass, concrete or sand are not statistically different at $p \leq 0.05$, primarily for two reasons: (i) the calculated *p*-values (0.419 for grass) appear to be much larger than the probability level at 5%; and (ii) the F-ratio between groups and within groups (0.879) is much smaller than the F-critical (3.101) for the grass area. The same trends can be observed for the Concrete and Sand surfaces in Table 2a.

The means of the wet-bulb temperatures measured by the Kestrel and Sling Psychrometer (control groups) and by the IR Thermometer (test group) for grass, concrete or sand shown in Table 2b are also not statistically different at $p \leq 0.05$ for two reasons similar to those of the dry-bulb cases: (i) the calculated *p*-values (0.367 for Grass) appear to be much larger than the probability level at 5%; and (ii) the F-ratio between groups and within groups (1.015) is significantly smaller than the F-critical (3.105) for the grass surface. The same trends are seen for the concrete and sand surfaces in Table 2b.

3.3. Dry- and Wet-Bulb Temperature Measurements over Grass, Concrete and Sand Surfaces

The statistical data analysis of the experimental results shows that the IR Thermometer and wet paper towel technique described here can reliably quantify wet-bulb temperature compared to direct psychrometric and Kestrel wet-bulb measurements. Although cloud cover and a slight breeze provided ideal conditions, the IR Thermometers proved to be fast and effective for wet-bulb temperature measurements in nearly all conditions. Figures 2–4 show that dry- and wet-bulb temperatures measured by the IR Thermometer align well with the control Kestrel and Sling Psychrometer data sets, with an average difference of less than 5%. Note that data from the freezer experiments are not included in this <5% difference. Deviations from the control measurements can be partially attributed to solar heating contamination associated with man-made shading from direct sunlight, more specifically over the sand surface site due to the lack of shade and the utilization of a dark-colored (black) umbrella to shield the instrumentation from sunlight. Partly cloudy days also led to atmospheric and solar irradiance variability on time scales which likely were shorter than the time required to make each measurement. As stated previously, the total time to conduct all measurements over any of the particular surfaces studied was approximately 30 min, leading to plenty of opportunities for changes in sky conditions. Additionally, instances with high winds in the vicinity created notable fluctuations in IR Thermometer readings. For example, trials ~30–40 were collected on 2 June 2020 when winds of 7.5 m s^{-1} (15 kt) gusting to 10 + m s^{-1} (20 + kt) were observed at a nearby airport and military base (see Appendix A for trial number to date/time mapping).

The IR Thermometer dry-bulb temperature peaks seen in Figures 2a, 3a and 4a at trials 20, 47 and 69 (8 May, 3 June and 11 June) are directly attributable to high solar irradiance during those trials, affecting both the actual temperatures of the emitting surface and the internal temperatures of the IR Thermometer (despite attempts to maintain shade). Neither the Kestrel nor the Sling Psychrometer air (dry-bulb) temperature measurements were as affected at these times. However, the wet-bulb temperature plots in Figures 2b, 3b and 4b show much smaller differences among the Kestrel, Sling Psychrometer and IR Thermometer values at trials 20, 47 and 69. This suggests that the IR Thermometer dry-bulb temperature differences are due to the emitting dry paper towel surface becoming significantly warmer than the air temperature on sunny days, rather than the IR Thermometer losing accuracy due to solar-irradiance-induced temperature gradients within the IR Thermometer.

As mentioned above, trials 30–40 (1 and 2 June) were affected by wind speeds higher than those usually recommended for stable Sling Psychrometer evaporative cooling. This is readily seen in the wet-bulb plots of Figures 2b and 3b (and relative humidity values as seen in Appendix A). The IR Thermometer values are significantly lower than those of the Kestrel and Sling Psychrometer. The authors postulate that the wet paper towel material can reach stable evaporative cooling at significantly lower ventilation rates than those required for a Sling Psychrometer because of the lower heat capacity and mass of the paper towel compared to the glass and alcohol in the Sling Psychrometer wet-bulb thermometer. Thus, although the high winds (up to 10 m s^{-1}) that occurred during trials ~30–40 were on the upper end of acceptable WMO ventilation rates for a Sling Psychrometer [2], such wind speeds were likely too high for the wet paper towel to remain at a steady temperature if water continued to evaporate from the material. It appears that ventilation rates of less than 5 m s^{-1} are more favorable for the IR Thermometer Psychrometric method described in this work.

The table in Appendix A captures the time required in each trial to obtain a steady-state wet-bulb temperature measurement for each instrument. In all trials, the Sling Psychrometer required at least two minutes of slinging at about two revolutions per second to arrive at a steady wet-bulb temperature. The Kestrel and IR Thermometer required much less time to measure a wet-bulb temperature—usually about 30 s—but the Kestrel did have a few trials that required more than 90 s to reach a steady wet-bulb temperature. In all trials, the Sling Psychrometer required more time to obtain a steady dry-bulb temperature than the Kestrel and IR method. Overall, using the IR Thermometer Psychrometer was the fastest way to measure wet-bulb and dry-bulb temperatures. The Kestrel did provide instantaneous moisture parameter (e.g., relative humidity, vapor pressure, dew point) calculations that were not automatically derived with the Sling Psychrometer or IR Thermometer Psychrometer.

To obtain dew point temperatures from wet- and dry-bulb temperatures, psychrometric calculations, such as those outlined in Section 2.2; psychometric tables; or a psychrometric whiz wheel, such as that shown in Figure 6, must be used. The Bacharach Sling Psychrometer has a psychrometric slide-rule as part of the instrument, but this simple tool assumes a constant (presumably sea-level) pressure and a constant L_v, thus leading to inaccuracies. As such, the built-in Bacharach slide-rule tool was not used in this study. Appendix A lists the dew point temperatures as calculated from wet- and dry-bulb temperatures measured by the Sling Psychrometer and the IR Thermometer, or as read directly from the Kestrel. The dew point values are plotted in Figure 7 for all instruments with lines connecting the trial data points to allow the differences to be more easily seen. The Kestrel-displayed dew point temperatures were derived via the Kestrel's built-in algorithm. As is evident in Figure 7, the USAF whiz wheel and the psychrometric equations in Section 2.2 provided virtually the same results. The USAF whiz wheel was predominantly used to obtain the dew point temperatures for the Sling Psychrometer. Figure 7 also shows the high wind scenario discrepancies noted previously. In particular, there were seven trials (32, 33–35, 37–39) in which high winds resulted in excessive evaporative cooling of the paper towel target and unreliable IR wet-bulb temperatures, which in turn led to poor dew point temperature and relative humidity calculations.

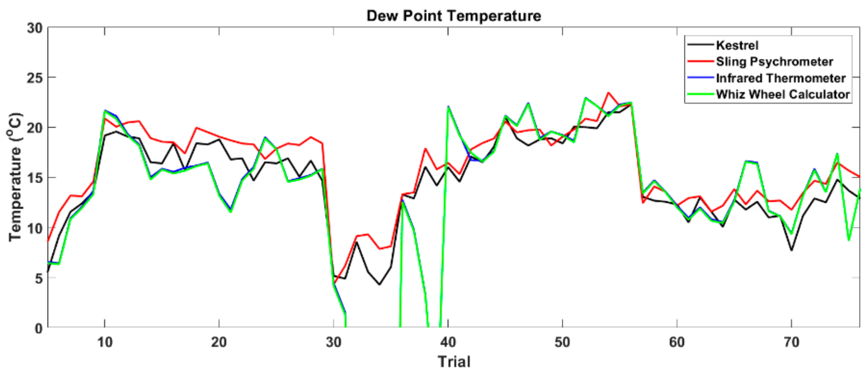

Figure 7. Dew point temperatures measured by the Kestrel (black) and derived from dry- and wet-bulb measurements collected by the Sling Psychrometer (red), infrared thermometer (blue) and whiz wheel calculator (green).

The possible utility of using IR Thermometers/detectors to evaluate moisture and heat fluxes near the surface was also explored in this research. In separate experiments, it was found that the IR sensor could be used to sense wet- and dry-bulb temperature changes of 0.7 °C and 0.6 °C over vertical distances as small as 50 cm, respectively. The results of these experiments using the Kestrel, IR Thermometer and paper towel pieces are shown in Figure 8. Lines are used to connect the data points across the trial times only to allow the differences between the values of each instrument to be more easily viewed. As referenced earlier, Figure 5 shows the vertical placement of the paper towels, and all data are available in Appendix A. The plots in Figure 8 demonstrate that both the Kestrel and IR Thermometer are able to discern the expected daytime near-ground temperature gradient—in which, over transpiring grass, the dry-bulb temperature is expected to rise slightly with height (in the first meter [8]). However, the transpiring grass should also result in greater moisture near the ground; therefore, the wet-bulb temperature should drop with height in the first meter above the surface [8]. Figure 8b shows that the IR Thermometer captures a significant drop with height in wet-bulb temperature. Interestingly, the Kestrel (Figure 8a) shows little or no change in wet-bulb temperature with height. Figure 9 isolates the measurements for the highest and lowest positions so that the vertical gradients are more easily discernible in the plots. Section 4 expands on these observations to outline the physical basis which permits use of the IR Thermometer Psychrometer for moisture flux measurements.

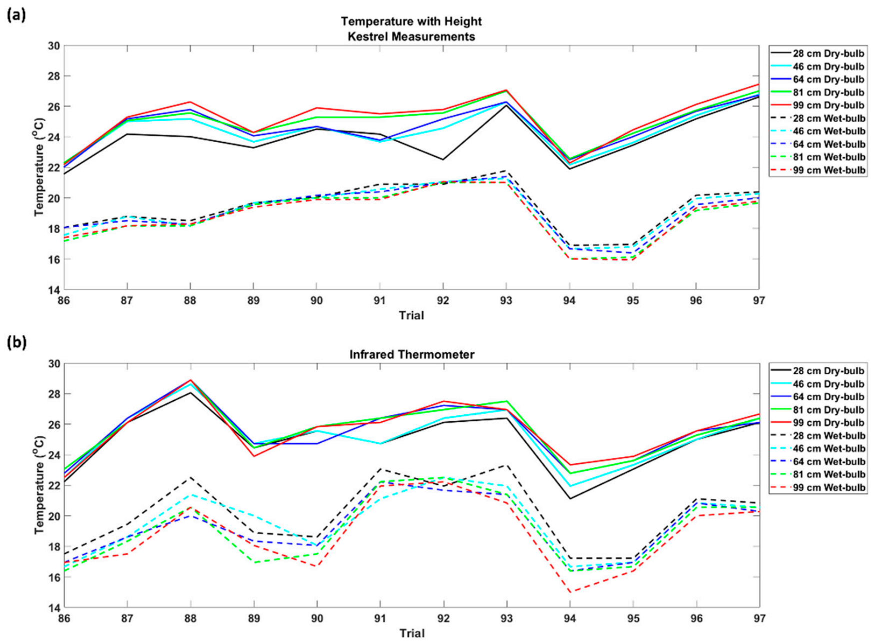

Figure 8. Vertical variations in dry-bulb (solid lines) and wet-bulb (dashed lines) temperatures measured by (**a**) the Kestrel and (**b**) the infrared thermometer at 28, 46, 64, 81 and 99 cm above a grassy surface. Note: the Sling Psychrometer was not used in this part of the experiment because it was impractical and unsafe to spin the device near the ground.

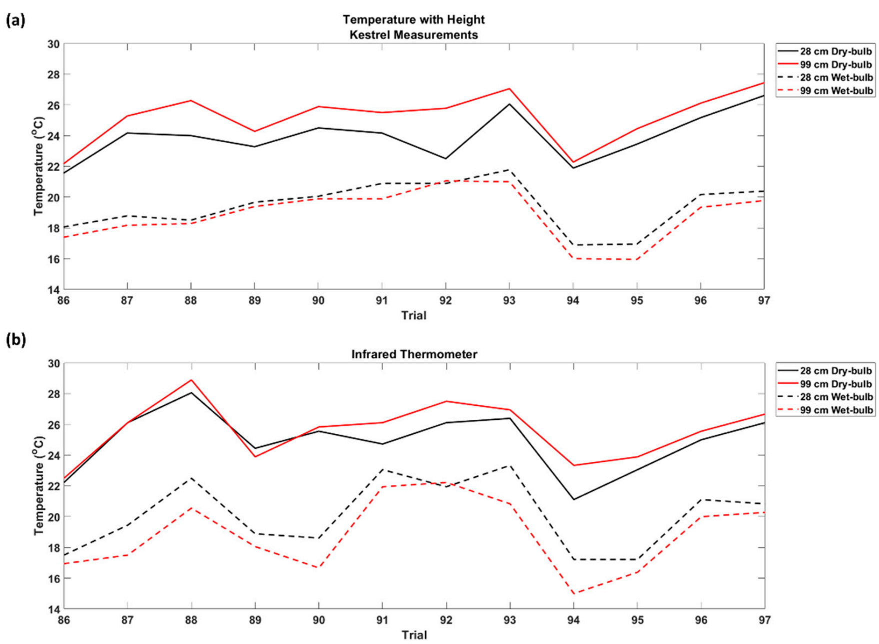

Figure 9. Vertical variations in dry-bulb (solid lines) and wet-bulb (dashed lines) temperatures measured by (**a**) the Kestrel and (**b**) the infrared thermometer at 28 and 99 cm above a grassy surface.

4. Potential Flux Measurement Method

The word 'flux' can be defined in very simple terms: how much of something passes through a unit area, or a unit volume, per unit time. For instance, if 100 birds fly through a 1×1 m^2 window each minute, then the flux of birds is 100 birds m^{-2} min^{-1}. If the window was 5×5 m^2, the flux would be 4 birds m^{-2} min^{-1}. Therefore, the flux is dependent on: (i) the number of things crossing an area/volume, (ii) the size of an area/volume being crossed and (iii) the time it takes to cross this area or pass through this volume. In more scientific terms, the flux can be defined as the amount of flow of a fluid, the amount of radiation or the number of particles incident through a flat surface in a given time [14–16]. Flux is also synonymously stated as flow rate per unit area. In transport phenomena (heat transfer, mass transfer and fluid dynamics), flux is defined as the rate of flow of a property per unit area, which has the dimensions [quantity]·[time]$^{-1}$ ·[area]$^{-1}$ [17].

There is a constant exchange of thermal energy, moisture (i.e., water vapor) and gases between the soil and the atmosphere. Atmospheric moisture is the resultant product of evapotranspiration and precipitation [14–16]. There are several procedures employed to measure heat and moisture flux. Their applications and usages are situational and, moreover, dependent on the nature of objects, equipment and resources. Each technique has its own advantages and disadvantages. Nonetheless, the proposed technique of using a handheld IR Thermometer for deriving the heat and moisture flux is inexpensive and easy to use for various ground and water surfaces, such as: a green and dry vegetation canopy, tree lines of a uniform surface/canopy, mixed vegetation with varying canopy heights, as well as seas, lakes, rivers and ponds. Although using an IR Thermometer to determine heat flux appears to be a relatively straightforward argument, using a standard handheld IR Thermometer to accurately evaluate moisture flux requires more discussion. The following suggests that the proposed use of an IR Thermometer Psychrometer indeed has merit.

Both sensible heat flux, Q_H and moisture flux, Q_E, (also called latent heat flux) can be quantified per unit area from vertical profile measurements of temperature and specific humidity [8,18]. These vertical profile gradients can be obtained from the dry- and wet-bulb IR temperature measurements, as demonstrated with the paper towels oriented in a vertical fashion as described in the previous section. Specific humidity can be calculated from the obtained vapor pressures and ambient pressure via

$$q = \frac{0.622e}{P - 0.378e}, \tag{6}$$

where q is the specific humidity of air vapor mixture, e is the vapor pressure and P is the atmospheric air pressure. According to Oke [8], Q_H and Q_E (W m^{-2}) are given by

$$Q_H = -\rho c_{pd} K_H \left(\frac{\partial \overline{T}}{\partial z} - \Gamma \right), \tag{7}$$

$$Q_E = -\rho L_v K_w \frac{\partial \overline{q}}{\partial z} \tag{8}$$

where ρ is the air density (kg m^{-3}), c_{pd} is the specific heat of dry air (J kg^{-1} K^{-1}) at constant pressure, K_H is the eddy conductivity or diffusivity for heat (m^2 s^{-1}), $\partial \overline{T}/\partial z$ is the vertical temperature gradient derived from the dry-bulb temperatures, Γ is the dry adiabatic lapse rate (-9.8 K km^{-1}), L_v is the latent heat of vaporization (J kg^{-1}), K_w is the eddy diffusivity for water vapor (m^2 s^{-1}) and $\partial \overline{q}/\partial z$ is the vertical moisture gradient derived from the wet-bulb temperatures. This method to obtain Q_H and Q_E, however, requires knowledge of K_H and K_w, which can vary significantly with location and environmental conditions.

Oke and Stull offer another method to quantify Q_H and Q_E that does not require values for the eddy diffusivities of heat and water vapor [8,18]. This is the Bowen's Ratio (β) method that combines the ratio of Q_H over Q_E with a measurement of the net all-wave radiation obtained by a net pyrradiometer device (Q^*) and with the ground/surface temperature flux (Q_G) measured with a ground heat flux plate or soil temperature probes at different depths. In this case, β can be found without K_H and K_w from:

$$\beta = \frac{Q_H}{Q_E} = \frac{c_{pd}\Delta\overline{T}}{L_v\Delta\overline{q}}, \tag{9}$$

and Q_H and Q_E are obtained from:

$$Q_H = \beta(Q^* - Q_G)/(1+\beta) \quad \text{and} \tag{10}$$

$$Q_E = \frac{Q^* - Q_G}{1+\beta} \tag{11}$$

According to previous research, which suggests the physical basis for applying an IR Thermometer for moisture flux measurements, Mzad successfully measured temperature gradients and heat flux using an IR Thermometer for tribological applications [19]. Perhaps the strongest published evidence indicating our proposed inexpensive and simple handheld IR Thermometer has definite merit for assessing moisture flux is that authored by Lee and Wang [10], and noted earlier in this paper. In the course of design and demonstration of a more efficient wick central to their digital psychrometer commonly used in greenhouses, Lee and Wang developed a comprehensive evaporative model using an IR digital thermometer to quantitatively track moisture flux in their instrument's captive wick, thus predicting when the wick's water reservoir needed to be filled. Although the ultimate objective herein is to use the proposed IR Thermometer Psychrometer to assess the moisture flux between the Earth's surface or surface canopy and the atmosphere, Lee and Wang highlighted the practicability of achieving relatively accurate moisture flux using an IR Thermometer and fundamental evaporative and psychrometric relationships. There are several interesting challenges to be explored using the IR Thermometer Psychrometer for earth–atmosphere moisture flux measurements, one of those being the determination of emissivity, with sufficient accuracy, for the various earth surface types that one is likely to encounter. To sum up the above, a combination of an IR Thermometer together with instrumentation to measure pressure (e.g., a Kestrel) appears to be an inexpensive alternative configuration with capabilities comparable to traditional soil/air moisture and temperature instrumentation suites normally employed for moisture flux measurements (see Appendix A of Oke [8]). In summary, the previous discussion supports the hypothesis that IR sensors/detectors can be used for determining near-surface moisture and heat fluxes.

5. Conclusions

This study describes a lower-cost, time-efficient method to obtain psychrometric wet- and dry-bulb temperatures using an infrared thermometer, hand-held fan and paper towels. It also demonstrates the viability of replacing multiple, vertically-stacked dry- and wet-bulb thermometers with a single non-contact IR temperature sensor to measure temperature and moisture gradients/fluxes in the first 1–2 m of the surface layer. The materials and tools used cost less than 50 USD total to acquire and operate. The IR technique to obtain the ambient air and wet-bulb temperatures was validated with Kestrel 4000 (discontinued; the Kestrel 5000 replacement typically costs 259 to 319 USD) and Bacharach Sling Psychrometer (typical cost: ~85 USD) measurements under various atmospheric conditions, as well as over different surface types to test the versatility of the method. Standard meteorological surface data were collected during each experiment, and moisture parameters were derived via psychrometric equations and were further compared to the results obtained with a USAF psychrometric whiz wheel. The IR method described herein was shown to be robust in many environmental settings—both indoors (see Appendix A, trials 54–62) and outdoors—if the IR Thermometer is shaded from direct sunlight, shielded from strong winds (>5 m s^{-1}) and in near equilibrium with its immediate surrounding environment. Moreover, wet-bulb measurements were on average −0.3 K different from the control Kestrel wet-bulb values. Significantly, when the seven trials with high winds are removed, this average Kestrel wet-bulb to IR wet-bulb difference is reduced to approximately the same average difference as it is when comparing Kestrel to Sling Psychrometer wet-bulb differences (<0.1 K). In general, it took at least two minutes of whirling/spinning the Sling Psychrometer to obtain a steady dry- and wet-bulb set of readings, whereas the IR Thermometer typically steadied in less than 30 s. Finally, the possible utility of using a single IR Thermometer/detector to evaluate moisture and heat fluxes near the surface was explored. Indeed, the case was made suggesting that the IR sensor can be used to sense wet- and dry-bulb temperature changes of 0.7 K and 0.6 K, respectively, over vertical distances as small as 50 cm, thus allowing surface layer temperature and moisture gradients/fluxes to be quantified. The feasibility of this single IR detector method to provide values of surface layer heat and moisture fluxes with reasonable certainty suggests the technique can be exploited with more efficiency and accuracy with a calibrated imaging IR camera or sensor array.

Author Contributions: Conceptualization, S.F.; methodology, S.F.; validation, S.F., L.T. and Y.R.; formal analysis, S.F., L.T., J.S. and Y.R.; investigation, L.T and J.M.; resources, S.F., L.T. and J.M.; data curation, S.F., J.S. and Y.R.; writing—original draft preparation, S.F., J.S., Y.R. and K.K.; writing—review and editing, S.F., J.S., Y.R., K.K. and J.M.; visualization, L.T., J.S. and Y.R.; supervision, S.F.; project administration, S.F.; funding acquisition, S.F. All authors have read and agreed to the published version of the manuscript.

Funding: This work was supported by the Joint Directed Energy Transition Office (DE-JTO).

Institutional Review Board Statement: Not applicable.

Informed Consent Statement: Not applicable.

Data Availability Statement: All experimental data collected and described in Section 3 can be found in Appendix A.

Acknowledgments: The authors would like to thank the Joint Directed Energy Transition Office for sponsoring this research through the Directed Energy Summer Intern (DESI) program. The views expressed in this paper are those of the authors and do not necessarily reflect the official policy or position of the Air Force, the Department of Defense or the U.S. Government.

Conflicts of Interest: The authors declare no conflict of interest.

Appendix A

The measured and derived experimental data from trials conducted in Dayton OH in June–July 2020 are shown. In addition to the date and time, sky conditions and surface types were documented to explore the versatility and limitations of the IR Thermometer technique.

						Kestrel							Sling Psychrometer						Infrared Sensor						Whiz Wheel (from IR Temperatures)		
Trial	Date	Time (EDT)	Time of Day	Sky Condition	Surface	Dry Bulb (°F)	Wet Bulb (°F)	RH (%)	Dew Point (°F)	Pressure (mb)	Lv	Specific Humidity	Dry Bulb (°F)	Wet Bulb (°F)	RH (%)	Dew Point (°F)	Lv	Specific Humidity	Dry Bulb (°F)	Wet Bulb (°F)	RH (%)	Dew Point (°F)	Lv	Specific Humidity	RH (%)	Vapor Pressure (mb)	Dew Point (F)
Assistant Aid																											
1	5/18/2020	10:30am	morning	overcast	concrete	70.5	65.1	74.4	62.2	N/A	N/A	N/A	69.5	66	N/A	N/A	N/A	N/A	73	66	N/A	N/A	N/A	N/A	N/A	N/A	N/A
2	5/18/2020	12:30pm	midday	overcast	concrete	66.7	62.7	80.5	60.6	N/A	N/A	N/A	63	63	N/A	N/A	N/A	N/A	67.5	63	N/A	N/A	N/A	N/A	N/A	N/A	N/A
3	5/18/2020	2:30pm	afternoon	overcast	concrete	67.1	63.5	81.2	61.5	N/A	N/A	N/A	65	64	N/A	N/A	N/A	N/A	68	64	N/A	N/A	N/A	N/A	N/A	N/A	N/A
4	5/18/2020	5:00pm	evening	overcast	concrete	62.2	57.3	76.2	55.4	N/A	N/A	N/A	60.5	59.5	N/A	N/A	N/A	N/A	62.5	56.5	N/A	N/A	N/A	N/A	N/A	N/A	N/A
5	5/20/2020	11:30am	midday	overcast	concrete	54.8	47.8	65.7	42	988.9	2472450	0.00552861	52	49.5	84.362	47.43419	2474825	0.00701228	50.5	47	77.698	43.8009	2477200	0.006109701	78.0%	9.65	43.6
6	5/21/2020	11:00am	morning	overcast	concrete	60.4	53	71.3	48.5	988.5	2464100	0.00695036	57	54.5	85.662	52.74999	2467700	0.00854824	58.5	50.5	57.489	43.5544	2465350	0.006054815	57.0%	9.52	43.4
7	5/21/2020	1:30pm	afternoon	overcast	concrete	60	56.8	74.2	52.8	987.8	2464100	0.00918924	59	57	88.846	55.71708	2465350	0.00953321	61	55.5	71.267	51.6402	2463000	0.008211601	70.5%	12.94	51.5
8	5/21/2020	4:30pm	afternoon	overcast	concrete	62.9	58.4	72.5	54.3	986.9	2460800	0.00949052	60.5	57.5	83.822	55.58698	2463000	0.00949696	62	57	74.168	53.6881	2463000	0.008861821	73.5%	13.88	53.5
9	5/22/2020	10:30am	morning	overcast	concrete	66.5	62	68.7	56.4	986.5	2457500	0.0109308	63	60	84.429	58.23563	2460650	0.01045396	67	60.5	69.233	56.5984	2453500	0.009855361	69.0%	15.24	56.0
10	5/26/2020	1:15pm	afternoon	mostly sunny	concrete	83.3	73	55.3	66.5	986.6	2434400	0.015107	85	74	59.945	69.55245	2429800	0.01553939	89	76	55.442	70.9958	2425050	0.016323348	55.0%	25.74	70.9
Whiteboard Setup																											
11	5/26/2020	2:30pm	afternoon	partly cloudy	grass	81.6	72.3	58.3	67.2	985.7	2434400	0.01494391	83	72.5	60.779	68.07704	2435750	0.01478585	89.5	75.5	52.748	69.9962	2425050	0.015791225	52.0%	24.72	69.5
12	5/27/2020	9:00am	morning	overcast	concrete	70.5	67.8	84.7	66.3	985.7	2450900	0.01403038	71	69.5	92.919	68.84947	2447600	0.01518353	74	69	78.091	66.7451	2447600	0.014121538	77.5%	22.18	66.5
13	5/27/2020	9:00am	morning	overcast	grass	71.9	67.4	82	66	985.6	2447600	0.01341977	70.5	69.5	95.226	69.06829	2450550	0.01529943	73	67.5	75.722	64.8905	2447600	0.013241594	75.5%	21.00	64.7
14	5/27/2020	12:00pm	midday	mostly sunny	concrete	80	68.3	46.9	61.7	985.2	2437700	0.01222747	80.5	70.5	61.413	66.02579	2435750	0.01378079	87	68.5	38.88	59.0016	2429800	0.010759036	39.0%	16.59	58.6
15	5/27/2020	12:00pm	midday	mostly sunny	grass	82.9	67.6	51.9	61.5	985.1	2434400	0.01104462	78.5	69.5	64.128	65.38199	2441700	0.01347716	86	69	42.396	60.5357	2429800	0.011365049	42.0%	17.95	60.4
16	5/27/2020	4:00pm	afternoon	partly cloudy	concrete	82.5	71.7	47.1	65.1	983.3	2434400	0.01429735	85.5	71.5	50.867	65.25865	2429800	0.01344397	87	69	40.262	59.9807	2429800	0.011163219	40.0%	17.47	59.7
17	5/27/2020	4:00pm	afternoon	partly cloudy	grass	83.3	70.8	45.4	60.2	983.3	2434400	0.01340252	86	70.5	46.702	63.27399	2429800	0.01254241	82.5	68	47.756	60.7158	2435750	0.011458928	47.0%	17.68	60.2
18	5/28/2020	10:00am	morning	partly cloudy	concrete	72.6	66.9	79.8	65.1	982.6	2447600	0.01294196	71.5	69	88.407	67.8953	2447600	0.01473997	74	65.5	64.1	61.1087	2447600	0.011628081	64.0%	18.25	61.0
19	5/28/2020	10:00am	morning	partly cloudy	grass	73.2	66.5	76.5	64.9	982.7	2447600	0.01251657	70	68	90.497	67.09284	2450550	0.01433603	71.5	65	71.073	61.6425	2447600	0.011848729	71.0%	18.56	61.5
20	5/28/2020	2:30pm	afternoon	partly cloudy	concrete	84.5	72.5	50.4	65.8	982.7	2431100	0.01448923	80	70.5	62.983	66.28145	2438725	0.01393894	95	69.5	27.188	56.0258	2420300	0.00969056	27.0%	15.07	55.7
21	5/28/2020	2:30pm	afternoon	partly cloudy	grass	79.7	68.7	51.4	62.2	982.7	2437700	0.01263251	78	69.5	65.771	65.63481	2441700	0.01362944	89.5	66.5	29.137	53.2236	2425050	0.008749515	29.0%	13.61	52.7
22	5/28/2020	4:30pm	afternoon	partly cloudy	concrete	87.8	71.7	45.3	62.4	981.4	2427800	0.01310423	82.5	70.5	55.673	65.07605	2435750	0.01338457	86	68	39.673	58.675	2429800	0.010675158	39.5%	16.59	58.4
23	5/28/2020	4:30pm	afternoon	partly cloudy	grass	83.4	69.8	42.4	58.4	981.6	2434400	0.0126321	79.5	69.5	61.025	64.90248	2438725	0.0133011	85.5	69	43.566	60.8519	2429800	0.011534394	43.0%	17.98	60.5
24	5/28/2020	9:00pm	sunset	mostly cloudy	concrete	73.2	67.1	64.2	61.7	981.4	2447600	0.01296707	76.5	67	61.469	62.28485	2441700	0.0121367	78.5	70	65.981	66.2016	2441700	0.013918808	65.5%	21.81	66.0
25	5/28/2020	9:00pm	sunset	mostly cloudy	grass	76.2	66.9	60.3	61.5	981.5	2444300	0.01213385	74.5	67.5	70.175	64.15591	2447600	0.01295998	79.5	69	59.246	64.0558	2429800	0.01291467	59.0%	20.32	64.0
Chair Setup																											
26	5/29/2020	11:00am	morning	mostly cloudy	concrete	72.8	67.8	65	62.4	983	2447600	0.01354511	69.5	66.5	85.802	65.06567	2453500	0.01335795	68.5	62	69.907	58.303	2453500	0.010516562	69.5%	16.56	58.2
27	5/29/2020	11:00am	morning	mostly cloudy	grass	70.8	63.6	67.2	59.1	982.5	2450900	0.01105687	68.5	66	87.948	64.7911	2453500	0.01323737	70.5	63	66.535	58.8326	2450550	0.010723529	66.0%	16.83	58.6
28	5/29/2020	2:00pm	afternoon	mostly cloudy	concrete	81.6	69	56.3	62	981.3	2434400	0.01244071	73.5	68.5	77.982	66.22008	2447600	0.01392915	78.5	66	51.973	59.4208	2441700	0.010964851	51.5%	17.24	59.3
29	5/29/2020	2:00pm	afternoon	mostly cloudy	grass	73.7	64.2	60.5	58.4	981.5	2447600	0.0108129	71	67	81.632	65.10391	2450550	0.01339621	70.5	64	70.712	60.54	2450550	0.011408482	70.5%	17.98	60.5
30	6/1/2020	11:00am	morning	sunny	concrete	65.6	53.4	41.3	41.3	995.3	2457500	0.00592302	69	53.5	34.399	39.78573	2453500	0.00519945	63	51	42.666	39.9666	2460650	0.005236171	42.0%	8.23	39.5
31	6/1/2020	11:00am	morning	sunny	grass	66.7	52.7	41.6	40.8	995.5	2457500	0.00529181	63.5	52.5	47.345	43.116	2458300	0.00591212	65	50	32.376	34.7325	2458300	0.004260673	32.0%	6.71	34.3
32	6/1/2020	2:00pm	afternoon	partly cloudy	concrete	78.8	60.9	32.2	47.4	993.1	2437700	0.00732045	74	59	40.376	48.42417	2444650	0.00724698	71	44.5	1.2987	-29.792	2450550	0.000210638	0.80%	0.20	-32.6
33	6/1/2020	2:00pm	afternoon	partly cloudy	grass	74.6	60.6	30.8	42	993.1	2444300	0.00810138	71	58	45.226	48.747	2450550	0.00733508	62.5	43	12.209	9.5619	2460650	0.001475455	11.5%	2.20	10.5
34	6/1/2020	4:30pm	afternoon	partly cloudy	concrete	78.6	62.7	24.6	39.7	991.4	2437700	0.00854959	74	58	37.044	46.13655	2444650	0.00666042	85	54.5	8.0581	17.3206	2429800	0.002078756	7.80%	3.15	17.8
35	6/1/2020	4:30pm	afternoon	partly cloudy	grass	82.9	59.5	21.9	42.9	991.3	2434400	0.00551814	73.5	58	38.344	46.60439	2447600	0.00677992	78	47.5	0.1866	-58.6229	2441700	3.8329E-05	0.10%	0.04	-59.1
36	6/2/2020	11:30am	morning	sunny	concrete	77.9	64.5	45.9	55.9	985.6	2437700	0.00999313	78	64	46.63	55.94704	2441700	0.0096345	78	63.5	44.997	54.9658	2441700	0.009297164	44.0%	14.53	54.6
37	6/2/2020	11:30am	morning	sunny	grass	79.1	64.5	42.7	55.2	985.3	2437700	0.00972226	77.5	64	47.974	56.27541	2441700	0.00975274	79.5	61.5	35.171	49.6165	2438725	0.007637046	35.0%	11.99	49.4
38	6/2/2020	2:00pm	afternoon	sunny	concrete	83.8	69	44.3	60.9	984	2434400	0.01189408	82.5	70	54.03	64.21819	2435750	0.01295525	84.5	59	19.205	38.038	2429800	0.004911996	19.0%	7.72	37.9
39	6/2/2020	2:00pm	afternoon	sunny	grass	83.3	67.2	41.8	57.5	983.9	2434400	0.0106791	83	68	46.51	60.42765	2435750	0.0113353	77	50.5	9.2077	14.385	2441700	0.001843727	8.80%	2.74	15.0
40	6/2/2020	4:15pm	afternoon	sunny	concrete	85.8	71.2	43.7	60.8	982.5	2431100	0.01315251	87.5	70	41.937	61.57634	2429800	0.01182346	91	77	53.443	71.7665	2422675	0.016825866	53.0%	26.38	71.6
41	6/2/2020	4:15pm	afternoon	sunny	grass	85.4	69.2	39.3	58.2	982.4	2431100	0.01169815	84.5	68	42.974	59.5658	2432775	0.0110094	89.5	73.5	47.134	66.723	2425050	0.014158154	47.0%	22.32	66.5
42	6/3/2020	10:30am	morning	sunny	sand	77.3	68.5	59.8	62.7	980.2	2437700	0.01307108	78	68.5	62.161	64.0172	2441700	0.01291431	78.5	67.5	57.103	62.0723	2441700	0.012060762	60.0%	19.95	63.4
43	6/3/2020	10:30am	morning	sunny	grass	80.6	67.6	52.6	61.7	979.8	2437700	0.01165489	79	69.5	62.588	65.15681	2438725	0.01344421	77	67	59.906	62.0254	2441700	0.012045735	59.5%	18.79	61.8
44	6/3/2020	10:30am	morning	sunny	concrete	82	69.8	55.6	64.5	980.1	2434400	0.0129773	79	70	64.372	65.96441	2438725	0.013823	77	68	63.543	63.7002	2441700	0.012772955	63.5%	20.05	63.6
45	6/3/2020	1:00pm	midday	partly cloudy	concrete	80.6	73	62.4	69.8	980.4	2437700	0.0158391	84.5	73.5	59.81	69.0174	2432775	0.01535377	87.5	75	56.366	70.0865	2427425	0.015925594	56.0%	25.03	70.0
46	6/3/2020	1:00pm	midday	partly cloudy	grass	84.3	71.7	54.5	66	980.2	2431100	0.0139337	83.5	72	57.758	67.06743	2432775	0.01435998	82.5	72.5	62.303	68.3265	2435750	0.014996927	62.0%	23.47	68.2
47	6/3/2020	4:30pm	afternoon	partly cloudy	sand	87.9	72.5	47.4	64.7	978.4	2427800	0.0137794	88	73.5	50.687	67.45395	2427425	0.01457972	99.5	79.5	41.973	72.3611	2413150	0.017239884	42.0%	26.99	72.2

Figure A1. Experimental data conducted in Dayton OH in June–July 2020, Trials 1–47.

48	6/3/2020	4:30pm	afternoon	partly cloudy	grass	88.7	73.4	46.5	65.8	978.3	2427800	0.0143379	86	73	54.2	67.55141	2429800	0.01463032	84	71.5	54.818	66.0244	2432775	0.01387731	54.0%	21.64	65.7
49	6/4/2020	9:15am	morning	partly cloudy	sand	76.4	70.5	66.8	66	979.3	2444300	0.0148222	75	68	70.367	64.71269	2444650	0.01324433	78	70.5	69.512	67.2315	2441700	0.01445487	69.0%	22.66	67.2
50	6/4/2020	9:15am	morning	partly cloudy	grass	79.1	69.8	60.7	65.1	979.3	2437700	0.0136582	75	69	74.337	66.29006	2444650	0.01399151	76	69.5	72.665	66.5964	2441700	0.01414083	72.5%	22.28	66.5
51	6/4/2020	9:15am	morning	partly cloudy	concrete	80.2	71	62.6	68.1	979.1	2437700	0.0143435	75.5	70	76.497	67.60139	2444650	0.01464359	76.5	69	68.972	65.5726	2441700	0.01364999	68.0%	21.27	65.3
52	6/4/2020	12:00pm	midday	partly cloudy	concrete	76.8	70.8	74.7	68	979.5	2444300	0.0149620	78	72	75.224	69.52892	2441700	0.01563944	81.5	75.5	76.162	73.2747	2435750	0.01775953	76.5%	27.90	73.2
53	6/4/2020	12:00pm	midday	partly cloudy	grass	79.8	71.7	67.2	67.8	979.4	2437700	0.0149859	79	72	71.713	69.09533	2438725	0.01541055	81.5	74.5	72.481	71.8082	2435750	0.01690304	72.5%	26.65	71.8
Freezer Test																											
54	6/5/2020	10:30am	morning	freezing	freezer	32	19.1	45.1	21.6	971.8	2500900	-0.0005907	N/A	N/A	N/A	N/A	N/A	N/A	36	33.5	78.343	29.9195	2496200	0.00359580	78.0%	5.55	29.8
55	6/5/2020	12:00pm	midday	freezing	freezer	19.6	13	43.1	12.8	972.2	2500900	0.0002824	N/A	N/A	N/A	N/A	N/A	N/A	26.5	36	214.76	45.8114	2500900	0.00670885	N/A	N/A	N/A
56	6/5/2020	1:30pm	afternoon	freezing	freezer	36.1	28.3	58.3	25.6	971.7	2500900	0.0016246	N/A	N/A	N/A	N/A	N/A	N/A	33.5	29	59.157	20.7684	2498550	0.00245822	58.0%	3.69	21.2
57	6/8/2020	9:30am	morning	freezing	freezer	11.3	9.9	35.7	-9.4	977.5	2500900	0.0012093	N/A	N/A	N/A	N/A	N/A	N/A	20	28	215.26	38.7831	2500900	0.00509107	N/A	N/A	N/A
58	6/8/2020	12:30pm	midday	freezing	freezer	8.8	3.8	34.5	-10.1	977.2	2500900	3.798E-05	N/A	N/A	N/A	N/A	N/A	N/A	21.5	27	174.53	35.0787	2500900	0.00440065	N/A	N/A	N/A
59	6/8/2020	4:00pm	afternoon	freezing	freezer	16.2	9	36	-7.9	975.1	2500900	-0.0001421	N/A	N/A	N/A	N/A	N/A	N/A	22.5	29.5	192.95	38.6932	2500900	0.00508568	N/A	N/A	N/A
60	6/9/2020	1:00pm	midday	freezing	freezer	24.5	21.4	51.8	9.2	971.7	2500900	0.0018329	N/A	N/A	N/A	N/A	N/A	N/A	25.5	30	153.82	36.1225	2500900	0.00461261	N/A	N/A	N/A
61	6/9/2020	2:15pm	afternoon	freezing	freezer	30.2	22.7	47.9	17.6	971.2	2500900	0.0009944	N/A	N/A	N/A	N/A	N/A	N/A	27.5	30	127.9	33.5625	2500900	0.00416796	N/A	N/A	N/A
62	6/9/2020	3:00pm	afternoon	freezing	freezer	29.3	21.4	45.8	9.4	971	2500900	0.0007631	N/A	N/A	N/A	N/A	N/A	N/A	27.5	32	150.94	37.7398	2500900	0.00491984	N/A	N/A	N/A
Chair Setup																											
63	6/10/2020	10:30am	morning	cloudy	sand	78.8	73.7	74.4	70.7	976.4	2437700	0.0169046	79	75.5	85.336	74.22533	2438725	0.01839433	80	73	72.053	70.1933	2438725	0.01604920	72.0%	25.03	70.0
64	6/10/2020	10:30am	morning	cloudy	grass	81.5	73.4	69.9	70.7	976.1	2437700	0.0160415	78	73.5	81.14	71.75234	2441700	0.01692809	79	74	79.391	72.0819	2441700	0.01711805	79.0%	26.68	71.9
65	6/10/2020	10:30am	morning	cloudy	concrete	82	74.8	70.8	72.1	976.1	2437700	0.0171086	79	74	79.384	72.07945	2438725	0.01711665	80	74.5	77.694	72.4133	2438725	0.01731098	77.5%	27.13	72.4
66	6/11/2020	11:00am	morning	partly cloudy	sand	71.2	60.8	57.8	55.5	988.9	2450900	0.0090590	69	60	59.553	54.34725	2453500	0.00905956	69	61	63.69	56.1951	2453500	0.00968902	63.5%	15.31	56.1
67	6/11/2020	11:00am	morning	partly cloudy	grass	71.4	61.5	56.4	54.8	988.9	2450900	0.0094600	70	62	64.168	57.34926	2450550	0.01010145	72.5	63.5	61.374	58.4728	2447600	0.01051769	61.0%	16.59	58.3
68	6/11/2020	11:00am	morniing	partly cloudy	concrete	73.9	63.3	52	54.6	988.9	2447600	0.0100648	71.5	62	58.896	56.38849	2447600	0.00975708	71.5	62	58.896	56.3885	2447600	0.00975708	58.5%	15.44	56.3
69	6/11/2020	1:30pm	midday	sunny	sand	79.5	63.6	42	54.1	989.5	2437700	0.0089655	78	63	43.315	53.92168	2441700	0.00891439	79.5	63.5	41.162	53.8775	2438725	0.00889999	41.0%	14.02	53.6
70	6/11/2020	1:30pm	midday	sunny	grass	77	62	41.2	50.9	989.5	2437700	0.0084813	77.5	63.5	46.247	55.26479	2441700	0.00936179	74	60.5	45.634	51.7165	2447600	0.00822062	45.0%	12.90	51.4
71	6/11/2020	1:30pm	midday	sunny	concrete	80.4	65.8	41.3	55.4	989.5	2437700	0.0102697	78.5	64	45.26	55.57992	2441700	0.00946958	77	62.5	44.265	53.6101	2441700	0.00881335	44.0%	13.95	53.4
72	6/11/2020	4:00pm	afternoon	sunny	sand	81.8	64.4	36.4	52.8	989.7	2437700	0.0089775	79.5	63	39.617	52.83408	2438725	0.0085643	78.5	62	38.921	51.4603	2441700	0.00814154	38.5%	12.83	51.2
73	6/11/2020	4:00pm	afternoon	sunny	grass	80.2	63.6	36.2	50.1	989.4	2437700	0.0088065	78	63	43.297	53.9099	2438725	0.00891146	75	60.5	42.908	50.9567	2447600	0.00799365	43.0%	12.63	50.8
74	6/11/2020	4:00pm	afternoon	sunny	concrete	80.6	64.7	36.2	55	989.2	2437700	0.0094642	81	65.5	43.685	56.86501	2435750	0.00992356	79.5	64	42.723	54.8979	2438725	0.00924046	42.5%	14.53	54.6
75	6/12/2020	10:30am	morning	sunny	sand	73.5	61.7	49.9	53.2	993.6	2447600	0.0090509	72	61	53.344	54.13118	2447600	0.00894584	75.5	66.5	62.743	61.9226	2444650	0.01183535	62.5%	18.83	61.8
76	6/12/2020	10:30am	morning	sunny	grass	75.5	63.1	51	54.6	993.4	2444300	0.0095068	74	63	54.542	56.59774	2447600	0.00978666	74.5	66	64.208	61.6297	2447600	0.01171582	64.0%	18.56	61.4
77	6/12/2020	10:30am	morning	sunny	concrete	76.2	62.6	42.7	51.8	993.4	2444300	0.0090175	74	62	50.898	54.69245	2447600	0.00913278	75	61.5	46.236	52.9821	2444650	0.00857891	46.0%	13.65	52.9
78	6/12/2020	2:00pm	afternoon	sunny	sand	84.3	67.2	30.4	52.1	992.7	2431100	0.0103170	84	65.5	36.809	54.82416	2432775	0.00918318	95.5	68	23.135	52.0299	2416725	0.00828940	23.0%	13.21	52.0
79	6/12/2020	2:00pm	afternoon	sunny	grass	80.7	63.8	31.6	45.8	992.5	2437700	0.0087868	79	63	40.763	53.1632	2438725	0.00864395	77.5	60.5	36.561	48.8894	2441700	0.0073787	37.0%	11.75	48.8
80	6/15/2020	10:00am	morning	sunny	sand	67.4	58.2	59.9	52.1	995.1	2457500	0.0082602	63.5	59	77.081	56.19702	2458300	0.00962933	61.5	58	81.452	55.7742	2463000	0.00948289	81.5%	15.17	55.7
81	6/15/2020	10:00am	morning	sunny	grass	69.9	59.1	59.4	55.2	995.2	2450900	0.0082282	65.5	61	77.749	58.37531	2458300	0.01041464	67.5	63	78.36	60.5355	2453500	0.01124963	78.0%	17.85	60.3
82	6/15/2020	10:00am	morning	sunny	concrete	68.9	60.6	59.5	54.5	995.1	2450900	0.0093858	65	60.5	77.587	57.83225	2458300	0.01021454	66	60	70.971	56.326	2455900	0.00967438	71.0%	15.44	56.3
83	6/15/2020	1:00pm	midday	partly cloudy	sand	76.1	66	54	58.6	994.6	2444300	0.0113313	76	66.5	61.085	61.63668	2441700	0.01170457	84	70	49.954	63.3633	2432775	0.01243888	50.0%	19.84	63.3
84	6/15/2020	1:00pm	midday	partly cloudy	grass	78.2	62.9	54	56.6	994.4	2437700	0.0087361	71	64	68.698	60.20554	2450550	0.01112735	71	57.5	43.367	47.6277	2450550	0.00702442	43.5%	11.21	47.6
85	6/15/2020	1:00pm	midday	partly cloudy	concrete	73.7	62.4	51.5	55.2	994.4	2447600	0.0094491	71.5	63.5	64.816	59.05137	2450550	0.01067848	72	62.5	59.094	56.9504	2447600	0.00990215	59.0%	15.88	57.0
Vertical Orientation Test																											
86	6/16/2020	12:15pm	midday	partly cloudy	grass 28 cm	N/A	N/A	N/A	N/A	N/A	N/A	N/A	N/A	N/A	N/A	N/A	N/A	N/A	79.5	68.5	N/A	N/A	2438725	N/A	N/A	N/A	N/A
	6/16/2020	12:15pm	midday	partly cloudy	grass 46 cm	N/A	N/A	N/A	N/A	N/A	N/A	N/A	N/A	N/A	N/A	N/A	N/A	N/A	79.5	68	N/A	N/A	2438725	N/A	N/A	N/A	N/A
	6/16/2020	12:15pm	midday	partly cloudy	grass 64 cm	N/A	N/A	N/A	N/A	N/A	N/A	N/A	N/A	N/A	N/A	N/A	N/A	N/A	80.5	69	N/A	N/A	2435750	N/A	N/A	N/A	N/A
	6/16/2020	12:15pm	midday	partly cloudy	grass 81 cm	N/A	N/A	N/A	N/A	N/A	N/A	N/A	N/A	N/A	N/A	N/A	N/A	N/A	81	67	N/A	N/A	2435750	N/A	N/A	N/A	N/A
	6/16/2020	12:15pm	midday	partly cloudy	grass 99 cm	N/A	N/A	N/A	N/A	N/A	N/A	N/A	N/A	N/A	N/A	N/A	N/A	N/A	80.5	66.5	N/A	N/A	2435750	N/A	N/A	N/A	N/A
87	6/17/2020	9:30am	morning	sunny	grass 28 cm	70.8	64.5	54.8	55.9	991.5	2450900	0.0115494	N/A	N/A	N/A	N/A	N/A	N/A	72	63.5	63.067	58.7604	2447600	0.01059879	63.0%	16.86	58.7
	6/17/2020	9:30am	morning	sunny	grass 46 cm	71.9	63.6	54.1	55.9	991.5	2447600	0.0106885	N/A	N/A	N/A	N/A	N/A	N/A	72.5	62	55.568	55.7173	2447600	0.0094977	55.5%	15.14	55.6
	6/17/2020	9:30am	morning	sunny	grass 64 cm	71.6	64.5	54.1	55.7	991.5	2447600	0.0113650	N/A	N/A	N/A	N/A	N/A	N/A	73	62.5	55.855	56.3255	2447600	0.00970933	56.0%	15.54	56.3
	6/17/2020	9:30am	morning	sunny	grass 81 cm	72.1	62.9	53.6	55.2	991.5	2447600	0.0101776	N/A	N/A	N/A	N/A	N/A	N/A	73.5	61.5	50.611	54.0773	2447600	0.00894715	50.5%	14.29	54.1
	6/17/2020	9:30am	morning	sunny	grass 99 cm	71.9	63.3	53.2	54.8	991.5	2447600	0.0104883	N/A	N/A	N/A	N/A	N/A	N/A	72.5	62.5	57.473	56.684	2447600	0.00982339	57.5%	15.61	56.6
88	6/17/2020	12:30pm	midday	partly cloudy	grass 28 cm	75.5	65.8	46.4	55.5	990.5	2444300	0.0113843	N/A	N/A	N/A	N/A	N/A	N/A	79	67	53.794	60.8506	2438725	0.011430228	53.5%	18.15	60.8
	6/17/2020	12:30pm	midday	partly cloudy	grass 46 cm	77	65.8	44.3	35	990.5	2444300	0.0110417	N/A	N/A	N/A	N/A	N/A	N/A	79.5	65.5	47.47	57.8096	2438725	0.01025362	47.0%	16.25	57.6
	6/17/2020	12:30pm	midday	partly cloudy	grass 64 cm	77.3	65.3	43	55.2	990.5	2444300	0.0106244	N/A	N/A	N/A	N/A	N/A	N/A	79.5	65.5	47.47	57.8096	2438725	0.01025362	47.0%	16.25	57.6
	6/17/2020	12:30pm	midday	partly cloudy	grass 88 cm	77.1	64.7	42.5	54.8	990.5	2444300	0.0102563	N/A	N/A	N/A	N/A	N/A	N/A	79	65	47.163	57.173	2438725	0.010021264	47.0%	15.85	56.9
	6/17/2020	12:30pm	midday	partly cloudy	grass 99 cm	77.5	64.7	42.4	55.2	990.5	2444300	0.0101650	N/A	N/A	N/A	N/A	N/A	N/A	79	63.5	42.365	54.2163	2438725	0.009001779	43.5%	14.70	54.9
89	6/17/2020	3:30pm	afternoon	sunny	grass 28 cm	75.2	65.3	42.8	54.5	988.7	2444300	0.0111284	N/A	N/A	N/A	N/A	N/A	N/A	82.5	72.5	62.221	68.2879	2435750	0.01484829	62.0%	23.47	68.2
	6/17/2020	3:30pm	afternoon	sunny	grass 46 cm	77.3	64.7	42.2	54.5	988.7	2444300	0.0102345	N/A	N/A	N/A	N/A	N/A	N/A	83.5	70.5	52.874	64.5247	2432775	0.01303257	53.0%	20.66	64.5
	6/17/2020	3:30pm	afternoon	sunny	grass 64 cm	78.4	64.9	42	54.5	988.7	2437700	0.0101124	N/A	N/A	N/A	N/A	N/A	N/A	84	68	44.033	59.7971	2432775	0.011029868	44.0%	17.44	59.6
	6/17/2020	3:30pm	afternoon	sunny	grass 81 cm	78	64.7	41.1	54.3	988.7	2444300	0.0100746	N/A	N/A	N/A	N/A	N/A	N/A	84	69	47.001	61.6338	2432775	0.01177323	46.5%	18.52	61.4
	6/17/2020	3:30pm	afternoon	sunny	grass 99 cm	79.3	64.9	41	54.3	988.7	2437700	0.0099063	N/A	N/A	N/A	N/A	N/A	N/A	84	69	47.001	61.6338	2432775	0.01177323	46.5%	18.52	61.4
90	6/18/2020	12:00pm	midday	cloudy	grass 28 cm	73.9	67.4	58.7	60.9	987.4	2447600	0.0129372	N/A	N/A	N/A	N/A	N/A	N/A	76	66	59.33	60.8138	2441700	0.011451118	59.0%	18.12	60.7
	6/18/2020	12:00pm	midday	cloudy	grass 46 cm	74.6	67.4	57.4	61.1	987.4	2444300	0.0127753	N/A	N/A	N/A	N/A	N/A	N/A	76.5	68	65.111	63.9224	2441700	0.01277764	65.0%	20.25	63.9
	6/18/2020	12:00pm	midday	cloudy	grass 64 cm	75.3	67.2	57.1	61.3	987.4	2444300	0.0124705	N/A	N/A	N/A	N/A	N/A	N/A	76.5	65	54.21	58.7488	2441700	0.010638359	54.0%	16.76	58.6
	6/18/2020	12:00pm	midday	cloudy	grass 81 cm	75.7	67.2	56.9	61.1	987.4	2444300	0.0123791	N/A	N/A	N/A	N/A	N/A	N/A	76	62.5	46.982	54.3306	2441700	0.009067813	47.0%	14.29	54.2
	6/18/2020	12:00pm	midday	cloudy	grass 99 cm	75.7	66.9	56.9	60.4	987.4	2444300	0.0121629	N/A	N/A	N/A	N/A	N/A	N/A	75	64.5	57	58.7541	2444650	0.010640378	57.0%	16.80	58.6
91	6/18/2020	2:00pm	afternoon	cloudy	grass 28 cm	76.1	68.1	51.8	59.7	985.7	2444300	0.0129702	N/A	N/A	N/A	N/A	N/A	N/A	78	65.5	51.628	58.7733	2441700	0.010666064	53.0%	16.97	59.0
	6/18/2020	2:00pm	afternoon	cloudy	grass 46 cm	76.4	68	50.7	59.9	985.7	2444300	0.0128280	N/A	N/A	N/A	N/A	N/A	N/A	78	64.5	48.278	56.9072	2441700	0.009973971	47.0%	15.81	56.9
	6/18/2020	2:00pm	afternoon	cloudy	grass 64 cm	76.4	68.3	50.2	60.9	985.7	2444300	0.0130495	N/A	N/A	N/A	N/A	N/A	N/A	76.5	64.5	52.482	57.8458	2441700	0.010316969	52.0%	16.22	57.7
	6/18/2020	2:00pm	afternoon	cloudy	grass 81 cm	77.5	68	50.1	60.6	985.7	2437700	0.0125708	N/A	N/A	N/A	N/A	N/A	N/A	78.5	63.5	43.695	54.6126	2438725	0.009177368	43.5%	14.39	54.4
	6/18/2020	2:00pm	afternoon	cloudy	grass 99 cm	78.6	67.8	49.8	60.2	985.7	2437700	0.0121718	N/A	N/A	N/A	N/A	N/A	N/A	78.5	62	38.972	51.4958	2438725	0.008185294	39.0%	12.80	51.2

Figure A2. Experimental data conducted in Dayton OH in June–July 2020, Trials 48–91.

92	6/19/2020	11:30am	morning	sunny	grass 28 cm	75.5	69.6	63	63.6	986.7	2444300	0.0142154	N/A	N/A	N/A	N/A	N/A	N/A	76.5	73.5	86.963	72.3322	2441700	0.017078175	87.0%	27.02	72.2
	6/19/2020	11:30am	morning	sunny	grass 46 cm	74.6	69	59.5	62.6	986.7	2444300	0.0139675	N/A	N/A	N/A	N/A	N/A	N/A	76.5	70	72.771	67.1192	2441700	0.014290935	73.0%	22.62	67.0
	6/19/2020	11:30am	morning	sunny	grass 64 cm	74.8	68.7	56.5	63.1	986.7	2444300	0.0136972	N/A	N/A	N/A	N/A	N/A	N/A	79.5	72	69.962	68.8535	2438725	0.015170212	69.5%	23.77	68.5
	6/19/2020	11:30am	morning	sunny	grass 81 cm	77.5	68	55.6	62.7	986.7	2444300	0.0125617	N/A	N/A	N/A	N/A	N/A	N/A	79.5	72	69.962	68.8535	2438725	0.015170212	69.5%	23.77	68.5
	6/19/2020	11:30am	morning	sunny	grass 99 cm	77.9	67.8	56.1	62.6	986.7	2437700	0.0123173	N/A	N/A	N/A	N/A	N/A	N/A	79	71.5	69.791	68.3037	2438725	0.014886474	69.0%	23.40	68.1
93	6/19/2020	2:00pm	afternoon	partly cloudy	grass 28 cm	72.5	69.6	61.3	63.3	986	2447600	0.0149126	N/A	N/A	N/A	N/A	N/A	N/A	79	71.5	69.797	68.3061	2438725	0.014898262	69.0%	23.40	68.1
	6/19/2020	2:00pm	afternoon	partly cloudy	grass 46 cm	76.2	69.9	61.2	63.5	986	2444300	0.0142956	N/A	N/A	N/A	N/A	N/A	N/A	79.5	72.5	71.824	69.6201	2438725	0.015584857	72.0%	24.48	69.4
	6/19/2020	2:00pm	afternoon	partly cloudy	grass 64 cm	77.3	69.8	58.6	63.8	986	2444300	0.0139678	N/A	N/A	N/A	N/A	N/A	N/A	81	71	61.62	66.5935	2435750	0.014043355	61.0%	22.15	66.4
	6/19/2020	2:00pm	afternoon	partly cloudy	grass 81 cm	78	69.8	58.7	62.7	986	2437700	0.0138029	N/A	N/A	N/A	N/A	N/A	N/A	80.5	72.5	68.479	69.1834	2435750	0.015353675	68.0%	24.11	69.0
	6/19/2020	2:00pm	afternoon	partly cloudy	grass 99 cm	78.4	69.9	56.2	62.7	986	2437700	0.0137878	N/A	N/A	N/A	N/A	N/A	N/A	81.5	72	63.553	67.9595	2435750	0.014721655	63.0%	22.86	67.8
94	6/22/2020	1:30pm	midday	partly cloudy	grass 28 cm	78.9	71.2	59.7	65.3	982.3	2437700	0.0147453	N/A	N/A	N/A	N/A	N/A	N/A	79.5	74	77.53	71.8664	2437700	0.016886392	77.5%	26.62	71.8
	6/22/2020	1:30pm	midday	partly cloudy	grass 46 cm	79.3	70.3	59	65.3	982.3	2437700	0.0139496	N/A	N/A	N/A	N/A	N/A	N/A	80.5	71.5	64.946	67.6425	2437700	0.014616563	64.5%	22.86	67.4
	6/22/2020	1:30pm	midday	partly cloudy	grass 64 cm	79.3	70.5	59	65.4	982.3	2437700	0.0141049	N/A	N/A	N/A	N/A	N/A	N/A	80.5	70.5	61.452	66.0437	2437700	0.013830071	62.0%	21.67	65.9
	6/22/2020	1:30pm	midday	partly cloudy	grass 81 cm	80.6	69.8	57.4	65.8	982.3	2437700	0.0132664	N/A	N/A	N/A	N/A	N/A	N/A	81.5	70.5	58.495	65.5631	2437700	0.01360103	58.0%	21.17	65.2
	6/22/2020	1:30pm	midday	partly cloudy	grass 99 cm	80.7	69.8	57.9	63.1	982.3	2437700	0.0132435	N/A	N/A	N/A	N/A	N/A	N/A	80.5	69.5	58.03	64.399	2437700	0.013059985	57.5%	20.56	64.3
95	6/23/2020	10:30am	morning	sunny	grass 28 cm	71.4	62.4	56.1	56.3	980.6	2447600	0.0101430	N/A	N/A	N/A	N/A	N/A	N/A	70	63	68.417	59.1359	2450550	0.010861538	68.0%	17.00	59.0
	6/23/2020	10:30am	morning	sunny	grass 46 cm	71.9	62	55.5	55.5	980.6	2447600	0.0097668	N/A	N/A	N/A	N/A	N/A	N/A	71.5	62	59.006	56.44	2447600	0.009858012	57.0%	15.17	55.8
	6/23/2020	10:30am	morning	sunny	grass 64 cm	72.5	62	55.1	55.4	980.6	2447600	0.0096299	N/A	N/A	N/A	N/A	N/A	N/A	73	61.5	52.293	54.5113	2447600	0.00919109	52.0%	14.39	54.5
	6/23/2020	10:30am	morning	sunny	grass 81 cm	72.6	60.8	55.1	55.4	980.6	2447600	0.0088331	N/A	N/A	N/A	N/A	N/A	N/A	73	61.5	52.293	54.5113	2447600	0.00919109	52.0%	14.39	54.5
	6/23/2020	10:30am	morning	sunny	grass 99 cm	72.1	60.8	54.8	54.6	980.6	2447600	0.0089472	N/A	N/A	N/A	N/A	N/A	N/A	74	59	40.616	48.5826	2444650	0.007383032	40.0%	11.45	48.2
96	6/23/2020	2:00pm	afternoon	sunny	grass 28 cm	74.2	62.5	53.5	55.2	987.2	2444300	0.0094847	N/A	N/A	N/A	N/A	N/A	N/A	73.5	63	56.197	56.9603	2447600	0.009977936	57.0%	16.02	57.3
	6/23/2020	2:00pm	afternoon	sunny	grass 46 cm	74.5	62.2	52.8	54.7	987.2	2444300	0.0092197	N/A	N/A	N/A	N/A	N/A	N/A	74	62.5	52.782	55.6922	2444300	0.009530404	52.5%	15.07	55.6
	6/23/2020	2:00pm	afternoon	sunny	grass 64 cm	75.2	61.5	52.7	54.6	987.2	2444300	0.0086060	N/A	N/A	N/A	N/A	N/A	N/A	74.5	62.5	51.283	55.3602	2444300	0.009416193	51.0%	14.87	55.2
	6/23/2020	2:00pm	afternoon	sunny	grass 81 cm	75.6	61	52.1	53.2	987.2	2444300	0.0081944	N/A	N/A	N/A	N/A	N/A	N/A	74.5	62	49.503	54.3903	2444300	0.009089424	49.0%	14.32	54.4
	6/23/2020	2:00pm	afternoon	sunny	grass 99 cm	76	60.7	51.5	52.9	987.2	2444300	0.0079124	N/A	N/A	N/A	N/A	N/A	N/A	75	61.5	46.337	53.0418	2444300	0.008651717	46.0%	13.61	52.8
97	6/24/2020	11:00am	morning	partly cloudy	grass 28 cm	77.3	68.3	64.2	63.1	991.4	2444300	0.0127582	N/A	N/A	N/A	N/A	N/A	N/A	77	70	70.971	66.8748	2444300	0.014103509	70.5%	22.35	66.7
	6/24/2020	11:00am	morning	partly cloudy	grass 46 cm	77.7	67.9	63.5	63.2	991.4	2444300	0.0123730	N/A	N/A	N/A	N/A	N/A	N/A	77	69.5	69.057	66.086	2444300	0.013723264	69.0%	21.81	66.0
	6/24/2020	11:00am	morning	partly cloudy	grass 64 cm	78.2	67.2	63.3	62.8	991.4	2444300	0.0117503	N/A	N/A	N/A	N/A	N/A	N/A	78	69.5	65.698	65.6029	2444300	0.013494842	65.5%	21.50	65.6
	6/24/2020	11:00am	morning	partly cloudy	grass 81 cm	78.3	66.5	62.6	62.4	991.4	2444300	0.0112263	N/A	N/A	N/A	N/A	N/A	N/A	77.5	69	65.495	65.0397	2444300	0.01323277	65.5%	21.03	65.0
	6/24/2020	11:00am	morning	partly cloudy	grass 99 cm	79	66.8	61.8	62.5	991.4	2437700	0.0112728	N/A	N/A	N/A	N/A	N/A	N/A	78	68	60.259	63.1312	2444300	0.012377678	60.0%	19.64	63.0
98	6/24/2020	4:30pm	afternoon	partly cloudy	grass 28 cm	79.9	68.7	59.2	64.5	991.4	2444300	0.0124607	N/A	N/A	N/A	N/A	N/A	N/A	79	69.5	62.492	65.1125	2444300	0.013266419	61.0%	20.66	64.4
	6/24/2020	4:30pm	afternoon	partly cloudy	grass 46 cm	80.2	68.5	59	64.7	991.4	2444300	0.0122437	N/A	N/A	N/A	N/A	N/A	N/A	79.5	69	59.201	64.034	2444300	0.012775925	59.0%	20.25	63.9
	6/24/2020	4:30pm	afternoon	partly cloudy	grass 64 cm	80.1	68	59.1	63.9	991.4	2444300	0.0118980	N/A	N/A	N/A	N/A	N/A	N/A	79	68.5	58.965	63.4516	2444300	0.012517765	59.5%	20.25	63.9
	6/24/2020	4:30pm	afternoon	partly cloudy	grass 81 cm	80.6	67.4	57.8	63.2	991.4	2444300	0.0113466	N/A	N/A	N/A	N/A	N/A	N/A	79.5	69	59.201	64.034	2444300	0.012775925	59.0%	20.25	63.9
	6/24/2020	4:30pm	afternoon	partly cloudy	grass 99 cm	81.4	67.6	58	64	991.4	2437700	0.0113005	N/A	N/A	N/A	N/A	N/A	N/A	80	68.5	56.021	62.9275	2444300	0.012289342	56.0%	19.47	62.8

Figure A3. Experimental data conducted in Dayton OH in June–July 2020, Trials 92–98.

References

1. *Bacharach Sling Psychrometer Manual*; Rev. 7; Bacharach: New Kensington, PA, USA, 2017; Available online: https://www.instrumart.com/assets/Bacharach-Sling-Psychrometer-manual.pdf (accessed on 15 May 2020).
2. *Guide to Meteorological Instrumentation and Methods of Observation*, 7th ed.; WMO-No.8; World Meteorological Organization: Geneva, Switzerland, 2008; ISBN 978-92-63-100085.
3. Gruner, K.D. Principles of Non-Contact Temperature Measurements. Raytek Corporation. 2003. Available online: https://www.raytek.com (accessed on 3 July 2017).
4. Usamentiaga, R.; Venegas, P.; Guerediaga, J.; Vega, L.; Molleda, J.; Bulnes, F.G. Infrared Thermography for Temperature Measurement and Non-Destructive Testing. *Sensors* **2014**, *14*, 12305–12348. [CrossRef] [PubMed]
5. Riedl, M. *Optical Design Fundamentals for Infrared Systems*, 2nd ed.; SPIE Press: Bellingham, WA, USA, 2001.
6. Stephens, G.L. *Remote Sensing of the Lower Atmosphere: An Introduction*; Oxford University Press: Oxford, UK, 1994; p. 523.
7. Petty, G.W. *A First Course in Atmospheric Radiation*, 2nd ed.; Sundog Publishing: Madison, WI, USA, 2006; p. 459.
8. Oke, T.R. *Boundary Layer Climates*; Methuen and Co. Ltd.: London, UK, 1978; p. xxi+372.
9. Avdelidis, N.P.; Moropoulou, A. Emissivity considerations in building thermography. *Energy Build.* **2003**, *35*, 663–667. [CrossRef]
10. Lee, C.; Wang, Y.J. Psychrometer based on a contactless infrared thermometer with a predictive model for water evaporation. *Biosyst. Eng.* **2017**, *160*, 84–94. [CrossRef]
11. Fleagle, R.G.; Businger, J.A. *An Introduction to Atmospheric Physics*, 2nd ed.; Academic Press: New York, NY, USA, 1980.
12. Bolton, D. The Computation of Equivalent Potential Temperature. *Mon. Weather Rev.* **1980**, *108*, 1046–1053. [CrossRef]
13. Iribarne, J.V.; Godson, W.L. *Atmospheric Thermodynamics*; Springer: New York, NY, USA, 1973; p. 222.
14. Kaimal, J.C.; Finnigan, J.J. *Atmospheric Boundary Layer Flows: Their Structure and Measurement*; Oxford University Press: Oxford, UK, 1994; p. 289.
15. Swinbank, W.C. The measurement of vertical transfer of heat and water vapor by eddies in the lower atmosphere. *J. Meteorol.* **1951**, *8*, 135–145. [CrossRef]
16. Wyngaard, J.C. Scalar fluxes in the planetary boundary layer-theory, modeling, and measurement. *Bound.-Layer Meteorol.* **1990**, *50*, 49–75. [CrossRef]
17. Stauffer, P.H. Flux Flummoxed: A Proposal for Consistent Usage. *Groundwater* **2006**, *44*, 125–128. [CrossRef] [PubMed]
18. Stull, R. *An Introduction to Boundary Layer Meteorology*; Kluwer: Alphen Aan Den Rijn, The Netherlands; Springer: New York, NY, USA, 1988; p. 666.
19. Mzad, H. A simple mathematical procedure to estimate heat flux in machining using measured surface temperature with infrared laser. *Case Stud. Therm. Eng.* **2015**, *6*, 128–135. [CrossRef]